

PERFORMANCE ESTIMATION OF INDUCTION MOTOR DRIVE IN ELECTRIC TRACTION

A DISSERTATION

*Submitted in partial fulfilment of the
requirements for the award of the degree*

of

MASTER OF TECHNOLOGY

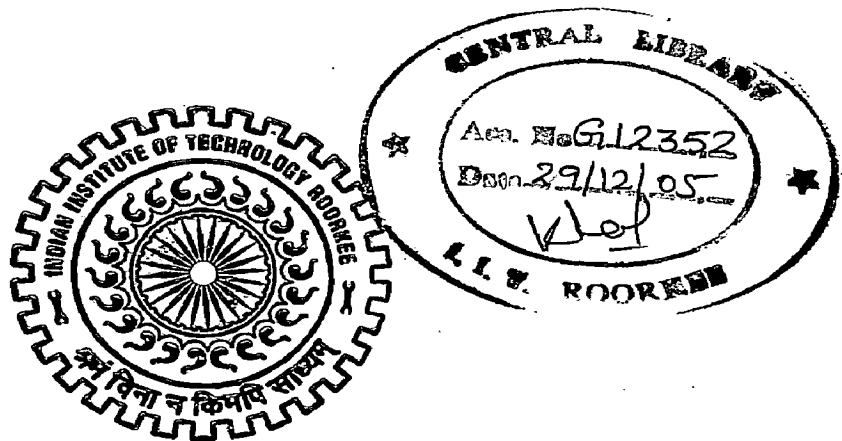
in

ELECTRICAL ENGINEERING

(With Specialization in Power Apparatus and Electric Drives)

By

DEEPAK KUMAR GOYAL



DEPARTMENT OF ELECTRICAL ENGINEERING
INDIAN INSTITUTE OF TECHNOLOGY ROORKEE
ROORKEE-247 667 (INDIA)

JUNE, 2005

CANDIDATE'S DECLARATION

I hereby declare that the work, which is being presented in the dissertation entitled "**Performance estimation of Induction Motor for Electric Traction**" in the partial fulfillment of the requirements for the award of degree of M. Tech. in the Power Apparatus and Electric Drives specialization, submitted in the Department of Electrical Engineering, IITR, Roorkee, is an authentic record of my own work carried out under the guidance of **Dr. S.P. Gupta**, Professor, Electrical. Engg. Deptt. and **Dr. S.P. Singh**, Associate Professor, Electrical Engg. Deptt, IITR, Roorkee.

The matter embodied in this dissertation has not been submitted by me for the award of any other degree or diploma of this institute or any other university/institute.


Date: 29 June, 2005



(Deepak Kumar Goyal)

Place: Roorkee

CERTIFICATE

This is to certify that the above statement made by the candidate is correct to the best of my knowledge and belief.


(Dr. S.P. Gupta)
Professor,
Electrical Engg. Deptt.,
IIT, Roorkee,
247667(India).


(Dr.S.P. Singh)
Associate Professor,
Electrical Engg. Deptt.,
IIT, Roorkee,
247667 (India).


ACKNOWLEDGEMENTS

I take this opportunity to express my sincere gratitude to **Dr. S. P.Gupta**, Professor, Electrical Engineering Department and **Dr. S.P.Singh**, Associate Professor, Electrical Engineering Department. IITR, for encouraging me to undertake this dissertation work as well as providing me all the necessary guidance and inspirational support throughout this work, without which this work would not have been in its present shape.

Special sincere heartfelt gratitude to my father, mother and family members, whose sincere prayer, best wishes, concern, support, unflinching encouragement and thoughtfulness has been a constant source of strength and upliftment to me during the entire work.

I thank all the members of Electrical Engineering Department for their help and encouragement at the hour of need.

Last, but not the least, I thank to Almighty God whose Divine Light provided me guidance, inspiration and strength to complete this work.


29/06/05

(Deepak Kumar Goyal)

Abstract

In the present work the performance of induction motor in traction system, which is fed by voltage source inverter, is investigated. The inverter is operated in space vector mode to make input and output current sinusoidal. The machine is modeled using d-q axis transformation. The transient and steady state performance of the induction motor is investigated for traction load. For obtaining speed control in whole speed range, a control scheme for Direct Torque Control and flux control (DTFC) of induction motor based on stator flux field-orientation method, is used.

LIST OF FIGURES

Figure No.	TITLE	Page No.
2.1	Switch model of a Three-phase Inverter.	12
2.2	Space Vector Diagram.	14
2.3	Construction of inverter space vector $V_1(100)$.	15
2.4	Construction of inverter space vector $V_2(110)$.	16
2.5	Construction of inverter space vector $V_3(010)$.	16
2.6	Construction of inverter space vector $V_4(011)$.	17
2.7	Construction of inverter space vector $V_5(001)$.	17
2.8	Construction of inverter space vector $V_6(101)$.	18
2.9	Symmetrical pulse pattern for three phase.	18
3.1	Idealized three phase Induction motor.	22
3.2	Connections and current conventions for a 3-phase Squirrel cage Induction motor.	23
3.3	Axes of a 3-phase symmetrical Induction motor .	23
3.4	Conventional per-phase equivalent circuit for a 3-phase, symmetrical Induction motor.	26
3.5	Arbitrary reference frame equivalent circuit for a 3-phase, symmetrical Induction motor.	28
	a) q-axis circuit.	
	b) d-axis circuit.	
3.6	Stationary reference-frame equivalent circuit for a 3-phase, symmetrical squirrel-cage Induction motor.	31

	a) d-axis circuit.	
	b) q-axis circuit.	
4.1	Block diagram of DTC of Induction motor.	36
4.2	Three-phase Inverter.	37
4.3	The Inverter output voltage corresponding to switching states.	39
4.4	Division of sector for stator flux linkage identification.	40
4.5	Effect of switching V_I and V_{VI} on stator-flux phasor.	41
5.1	Simulation block diagram.	46
5.2	Torque response when step change in load below base speed.	48
5.3	Rotor speed response when step change in load below base speed.	48
5.4	Stator phase current (I_{as}) response when step change in load below base speed.	49
5.5	Stator flux response when step change in load below base speed.	50
5.6	Stator flux sector response when step change in load below base speed.	50
5.7	Torque response when step change in speed below base speed.	51
5.8	Rotor speed response when step change in speed below base speed.	51
5.9	Stator phase current (I_{as}) response when step change in speed below base speed.	52
5.10	Stator flux response when step change in speed below base speed.	53
5.11	Stator flux sector response when step change in speed below base speed.	53

5.12	Torque response under traction type load below base speed.	54
5.13	Rotor speed response under traction type load below base speed.	54
5.14	Stator phase current (I_{as}) response under traction type load below base speed.	55
5.15	Stator flux response under traction type load below base speed.	56
5.16	Stator flux sector response under traction type load below base speed.	56
5.17	Torque response when step change in load above base speed.	58
5.18	Rotor speed response when step change in load above base speed.	58
5.19	Stator phase current (I_{as}) response when step change in load above base speed.	59
5.20	Stator flux response when step change in load above base speed.	60
5.21	Stator flux sector response when step change in load above base speed.	60
5.22	Torque response when step change in speed above base speed.	61
5.23	Rotor speed response when step change in speed above base speed.	61
5.24	Stator phase current (I_{as}) response when step change in speed above base speed.	62
5.25	Stator flux response when step change in speed above base speed.	63
5.26	Stator flux sector response when step change in speed above base speed.	63

5.27	Torque response under traction type load above base speed.	64
5.28	Rotor speed response under traction type load above base speed.	64
5.29	Stator phase current (I_{as}) response under traction type load above base speed.	65
5.30	Stator flux response under traction type load above base speed.	66
5.31	Stator flux sector response under traction type load above base speed.	66

LIST OF TABLES

Table No.	TITLE	Page No.
2.1	Summary of Inverter Switching States	14
4.1	Switching states of inverter phase lag a	38
4.2	Switching states of inverter phase lag b	38
4.3	Switching states of inverter phase lag c	38
4.4	Inverter switching states and machine voltage	39
4.5	Stator Flux Hysteresis Window output	41
4.6	Torque Hysteresis Window output	42
4.7	Switching states for possible S_λ , S_T and $S(k)$	43
4.8	Flux Phasor Sextants	43

CONTENTS

	Page No.
CANDIDATE'S DECLARATION	i
ACKNOWLEDGEMENT	ii
ABSTRACT	iii
LIST OF FIGURES	iv
LIST OF TABLES	viii
CONTENTS	ix
CHAPTER 1 : INTRODUCTION	1
1.1 Introduction	1
1.2 Traction motor	2
1.3 Traction Motor Control	3
1.4 Literature review	5
1.5 Organization of work	7
CHAPTER 2 : VOLTAGE SOURCE INVERTER AND SPACE VECTOR MODULATION	8
2.1 Introduction	8
2.2 PWM Voltage Source Inverter (PWM VSI)	8
2.3 PWM Techniques	9
2.3.1 Single Pulse Width Modulation Technique	9
2.3.2 Multiple Pulse Width Modulation Technique	9
2.3.3 Sinusoidal Pulse Width Modulation Technique	10

2.4 Space Vector Modulation	10
2.4.1 Introduction	10
2.4.2 Inverter Switching States	11
CHAPTER 3 : MATHEMATICAL MODELLING OF INDUCTION MOTOR	20
3.1 Development of the mathematical Model of Induction Motor	21
3.2 D-Q Model of Induction Motor	27
3.3 Motor equations in Arbitrary Reference Frame	27
3.4 Motor equation in Stationary Reference Frame	30
3.5 Per Unit System	32
CHAPTER 4 : DIRECT TORQUE CONTROL	34
4.1 Scalar control	34
4.2 Vector Control	34
4.3 Direct Torque Control	34
4.3.1 Introduction	35
4.3.2 Implementation Scheme	36
4.3.3 Switching State of Inverter	37
4.3.4 Flux Control	40
4.3.5 Torque Control	42
CHAPTER : 5 SIMULATION RESULTS AND DISCUSSION	45
5.1 Results and discussion in Constant Torque Region	45
5.1.1 Step change in load	45
5.1.2 Step change in speed	47
5.1.3 Traction type load	47

5.2 Results and discussion in Constant Power Region	57
5.1.1 Step change in load	57
5.1.2 Step change in speed	57
5.1.3 Traction type load	66
CHAPTER : 6 CONCLUSIONS AND SCOPE OF FURTHER WORK.	68
6.1 Conclusions	68
6.2 Scope of further work	68
BIBLIOGRAPHY	70
APPENDIX A : MACHINE PARAMETERS	

CHAPTER: 1

INTRODUCTION

1.1 INTRODUCTION

Many industrial applications require rotating electric motors. These motors are normally capable of speed control and often require an equipment to attain a versatile and smooth control and make the motor to operate on a desired speed and torque. These motors are characterized by the nature of speed torque characteristic such as constant torque motors or constant power motors. These are some time characterized by the type of motor used in the drive system, e.g., DC and AC motors, making use of dc and ac motor respectively. The variable speed application of a drive become more significant where a wide range of speed is required. Also precise control of speed is required for particular purpose and sometime regenerative braking is required in which kinetic energy of motor is returned to source. Thus, a drive should have precise speed control, should assure stable operation in complete range of speed and also should have good transient behaviour and good response to load change. Another desired feature of a drive is continuous, smooth and stepless control of speed very efficiently and economically [21].

Induction motor is used in AC drives. Both slip ring and squirrel cage induction motors are used. Squirrel cage induction motor has advantages that it is rugged, robust and has simple construction, lower cost, weight, volume and higher efficiency. It has large power/weight ratio as compared to dc motor. Since ac motor as constant speed motors, their speed control over a wide range is difficult. The speed of induction motor can be varied by

1. varying the stator voltage using a voltage controller
2. varying the rotor resistance using a chopper controlled resistance (for slip ring induction motor only).
3. slip energy recovery scheme (for slip ring induction motor only).
4. variable voltage variable frequency supply using VSI

1.2 TRACTION MOTOR

DC series motors are widely used in traction as principal drive motor. It has high starting torque and capability for high torque overloads. With an increase in torque, the flux also increases; therefore, for the same increase in torque, the increase in motor current is less compared to other motors. Thus during heavy torque overloads, power overload on the source and thermal overloading of motor are kept limited to reasonable values. The motor speed-torque is also suitable for better sharing of load between motors. Further, due to large inductance in field, sharp fluctuation in supply voltage do not produce sharp peaks in armature current thus motor commutation remain satisfactory, which does not happen in a separately excited motor, unless an additional inductor is connected in the armature circuit[10].

With the availability of semiconductor converter, separately excited motor is now preferred over series motor. With independent control armature and field, the speed-torque characteristic of separately excited motor can be shaped to satisfy the traction requirements in the optimum manner. Further, because of low regulation of its speed-torque characteristic, the coefficient of adhesion has higher value. On the other hand, series motor has a number of limitations. The field of a series motor can not be easily controlled by semiconductor switches. If the field control is not employed, the series motor must be designed with its speed equal to the highest desired speed of the drive. The higher base speeds are obtained by using fewer turns in the field winding. This however, reduces the torque per ampere at start and therefore acceleration. Further, there are a number of problems with regenerative and dynamic braking of a series motor. On the other hand, regenerative and dynamic braking of a separately excited motor are fairly simple and efficient, and can be carried out down to very low speed.

Currently compound motor is being preferred for traction applications as it incorporates the advantages of both series and separately excited motor.

Due to availability of reliable variable frequency semiconductor inverters, Squirrel cage induction motor is now finding applications in traction. Because of a number of advantages associated with this motor, this is likely to replace dc motors for traction applications.

Some of the important advantages of squirrel case induction motors over dc motors are ruggedness, lower maintenance, better reliability, lower cost, weight, volume and inertia, higher efficiency and ability to operate satisfactorily with sharp voltage fluctuation and in dusty environment. The major drawback of dc motor is the presence of commutator and brushes, which require frequent maintenance, particularly when the flashovers at the commutator occur due to sharp voltage fluctuations[10].

1.3 TRACTION MOTOR CONTROL

Operation of a dc separately excited motor for traction applications can be divided into three speed regions. First is constant torque region from zero to base speed. The field current is maintained constant at rated value and armature voltage is controlled in this region. Second is constant power region for above base speed. Here the armature voltage is maintained constant at rated value and field current is controlled. In both regions, the armature current is allowed to reach rated value on continuous basis. The limit of constant power operation is reached when a decrease in field current to increase motor speed leads to sparking at the brushes at the rated armature current. The motor is said to have reached commutation limit. Operation at higher speeds can now be carried out by progressively decreasing maximum allowable armature current. This is the third region of operation in which available output power of the motor progressively decrease with the increase in speed. Traction motor can be operated in third region because the torque required at high speed is much less compared to the accelerating torque[10].

The variable frequency controlled squirrel cage induction motors are also operated in three identical regions. Constant torque region from standstill to base speed with a constant v/f ratio and a constant maximum allowable stator current. Constant power region from base speed to the speed at breakdown torque limit is reached, here voltage and maximum allowable stator current are constant. For higher speeds, the motor operated in the third region where maximum allowable current is reduced inversely with speed, thus insuring that the motor torque does not exceed its breakdown value. Some important features of traction drives are;

1. Large torque is required during starting and acceleration in order to accelerate the heavy mass.

2. The motor is subjected to torque overload during acceleration and when negotiating up gradients.

The various control strategies, for the control of the inverter fed induction motor, have provided good steady-state but poor dynamic response. From the traces of the dynamic responses, the cause of such poor dynamic response is found to be that the air gap flux linkage deviate from their set values. The deviation is not only in magnitude but also in phase. The variations in the flux linkage have to be controlled by the magnitude and frequency of the stator and rotor phase currents and their instantaneous phase. So far, the control strategies have utilized the stator phase current magnitude and frequency. This resulted in the deviation of the phase and magnitudes of the air gap flux linkages from their set values.

The oscillation in the air gap flux linkage result in oscillations in electromagnetic torque and, if left unchecked, reflected as speed oscillations. This undesirable in many high performance application, such as in robotic actuators, centrifuges, servos, process drives, and metal-rolling mills, where high precision, fast positioning, or speed control are required. Such requirement will not be met with the sluggishness of control due to the flux oscillations. Further, air gap flux variation result in large excursions of stator currents, requiring large peak converter and inverter rating to meet the dynamic. An enhancement of peak inverter rating increase cost and reduces the competitive edge of ac drives in the marketplace, in spite of excellent advantages of the ac drive over dc drives.

Separately excited dc motors are simpler in control because they independently control flux and torque. This is made possible with separate control of field and armature current which, in turn, control the field flux and the torque independently. Moreover, the dc motor control requires only the control of the field or armature current magnitudes, providing simplicity which is not possible with ac motor control. By contrast, ac induction motors require a coordinated control of stator current magnitudes, frequency and their phase, but making it a complex control. As in the dc motors, independent control of flux and torque is possible in ac motors. The torque and flux is compared to reference torque and flux respectively, but this requires the position of the stator flux linkages at every instant, unlike in the dc machine. If this is available, then the control of ac

machines is very similar to that of separately-excited dc machines. The requirement of phase, frequency and magnitude control of the currents and hence of the flux phasor is made possible by inverter control. The control is achieved in field coordinates (hence the name of this control strategy is field oriented control) because it relates to the phasor control of the stator flux linkages.

Vector control made the ac drive equivalent to dc drives in the independent control of flux and torque and superior to them in their dynamic performance. These developments positioned the ac drives for high performance applications, hitherto reserved for separately excited dc motor drives.

1.4 LITERATURE REVIEW

T.G.Habetler, Deepakraj M. divan [1] presents a scheme for Direct torque Control of ac machine using discrete pulse-modulated inverters such as the resonant dc link inverter. A unique feature of the control method presented is that only one current sensor in the dc link is required. The scheme is of particularly important for realization of traction drive.

T.G.Habetler [2] presents a control scheme for Direct torque and Flux Control of induction machine based on the stator flux-orientation method. With the proposed predictive control scheme, an inverter duty cycle has directly calculated each fixed switching period based on the torque and flux error. This paper describes a method by which a voltage space vector can be calculated in order to control the torque and flux directly in a deadbeat fashion.

R.J. Hill [3] explains the electrical and control engineering background in electric railways. The articles cover traction drives with DC and AC traction motors.

R.J. Hill [4] described the nature of the traction load, the requirements of the traction duty cycle and power electronic controlled drives with DC traction motors. This article covers traction drives with inverter-fed three-phase induction motors.

Y.A.Chapuis, C.Pelissou, D.Roya [5] presents the Direct torque Control under square wave condition and proposed a control structure under square wave operation to optimize power and losses in the inverter and the machine.

Jun-Koo Kang and Seung-Ki Sul [8] present a direct torque control (DTC) method of an induction machine, which enables the minimum torque ripple control, while maintaining constant switching frequency.

P.S.Bimbhra[9] present different type of induction motor control schemes through PWM inverter. A general idea about Space Vector based voltage source inverter is also given.

G.K.Dubey[10] present the general idea about type of traction motor and about nature of load.

P. C. Krause [11] presents the induction motor model in different reference frame (stationary reference frame or arbitrary reference frame)

Yen-Shin Lai and Jian-Ho Chen [12] presents a new direct torque control technique based on the application of Space Vector Modulation for prefixed time intervals. In this way a sort of Discrete Space Vector Modulation is introduced.

Hu Hu, Yong Dong Li and Yi Zeng [13] presents a new stator flux estimation based on voltage model for direct torque control. The flux estimation, with simple structure, can observe the phase angle and amplitude of stator flux accurately and is robust to machine parameters variation in whole speed range.

Hu Hu Yongdong Li [14] presents the scheme of direct torque control for railways traction in whole speed range. It proposed that in low speed range , the locus of stator flux is controlled to be a circular to reduce torque ripple and in medium and high speed range, the locus of stator flux is controlled to be hexagonal to reduce switching frequency.

Qu wenlong, Yang yi [15] presents a control strategy of direct torque control of induction motor fed with GTO VSI applied to traction. Because the switching frequency

can not be high in the condition of high power GTO inverter application, different control method are adopted in different speed range.

B.K. Bose [16] presents the generalized space vector modulation technique for PWM inverter.

R. Krishnan [17] presents a implementation scheme of direct torque control for induction motor drives.

Nik Rumzi Nik Idris, and Abdul Halim Mohamed Yatim [18][19] presents a constant switching frequency torque controller which is capable of reducing the torque ripple and maintain a constant switching frequency.

1.5 ORGANISATION OF WORK

In the present work, the performance of VSI fed induction motor is estimated for the electric traction applications by simulation in MATLAB.

Chapter 1: Gives introduction of VSI fed drives, about speed control of induction motor and requirement of traction application. Literature review and work of organization is also presented in this chapter.

Chapter 2: Gives the basic idea of vsi and pwm technique and svm technique.

Chapter 3: Presents the mathematical modeling of induction motor, which is used in the simulation for traction purpose.

Chapter 4: Gives the basic scheme used for speed control of induction motor and software developed for the simulation purpose of the drive

Chapter 5: Discussion the results obtained with simulation.

Chapter 6: Conclude the results and suggest further work.

CHAPTER 2: VOLTAGE SOURCE INVERTER AND SPACE VECTOR MODULATION

2.1 INTRODUCTION

In modern industrial world induction motor is the most preferred motor for general purpose applications, due to low maintenance, high reliability and low cost. On account of these highly desired properties of induction motor an attempt has continued to employ induction motor in other areas of application. These applications may require high starting torque, smooth speed control. In almost industrial application speed control is required. For smooth speed control of an induction motor v/f control is the established method. In such applications the variable frequency supply can be generated by using static inverter, employing solid state power switching devices.

The supply generated by these inverter is usually non-sinusoidal in nature; i.e. there is presence of harmonics which gives rise to different undesirable effects in the machine, like torque pulsation, additional power losses, temperature rise etc. The inverter control of three phase six step inverter is simple and the switching loss is low as there are only six switching per cycle of fundamental frequency. However, the low order harmonics of the six step voltage wave will cause large distortion of current unless filtered by bulky and uneconomical low pass filter. It is possible to control the output as well as optimize the harmonics by performing multiple switching within the inverter with the constant dc input voltage.

2.2 VOLTAGE SOURCE INVERTER (VSI)

A Voltage Source Inverter is characterized by the stiff dc voltage supply at the input terminal of inverter and voltage source have negligible source impedance. The dc supply voltage may be fixed or variable, and may be obtained from utility power supply. In VSI the power semiconductor devices always remain forward biased due to the dc supply voltage. And therefore some type of force commutation is mandatory when using thyristors. Voltage source inverter can be classified as[9]:

- a) Square wave inverter, which may be of 180 degree of conduction or 120 degree of conduction.
- b) Twelve-step Inverter.
- c) Pulse Width Modulated Inverter.

2.3 PWM TECHNIQUES

Induction machines fed by non-sinusoidal supply have different harmonics in the current, which causes torque pulsation, heating, reduced efficiency and poor power factor. It is difficult to filter out the low frequency harmonics. These harmonics can be filter out by supplying machine with number of pulses per half cycle in the input voltage by Static switches. Thus, the process in which the voltage is controlled by varying the pulses during per half cycle is known as Pulse Width Modulation (PWM). Commonly used PWM techniques are,

- a) Single Pulse Width Modulation Technique.
- b) Multiple Pulse Width Modulation Technique.
- c) Sinusoidal Pulse Width Modulation Technique.

2.3.1 Single Pulse Width Modulation Technique

In Single Pulse Width Modulation control, there is only one pulse per half cycle and width of the pulse is varied to control the inverter output voltage. The gating signal is generated by comparing a rectangular reference signal of amplitude A_r with a triangular carrier wave of amplitude A_c . the frequency of the reference signal determines the fundamental frequency of output voltage. By varying A_r from 0 to A_c , the pulse width δ , can be varied from 0 to 180 degree. The ratio A_r to A_c control variable and defined as the amplitude modulation index. In this modulation, the dominant harmonics is the third and distortion factor increase significantly at a low output.

2.3.2 Multiple Pulse Width Modulation Technique

In Multiple Pulse Width Modulation, there are several pulses per half cycle of voltage. By comparing the triangular carrier wave with a reference wave generates the

gating signal for ON and OFF static devices. The modulation induction controls the output voltage. This type of modulation is also known as uniform pulse width modulation. The number of pulses per half cycle is determine by

$$P=m_f/2.0$$

Where m_f is modulation index. The variation of modulation index from zero to one varies and the width pf pulse from zero to π/P and the output voltage from zero to V_s . the distortion factor is reduce significant but due to large number of ON and OFF of static switches the switching losses in inverter increase.

2.3.3 Sinusoidal Pulse Width Modulation Technique

Most of the ac motors are designed to operate on a sine wave supply, and the inverter output should be as nearly sinusoidal as possible. Therefore, the three-phase square wave reference is replaced by a three-phase sinusoidal reference wave, to give a PWM waveform in which the pulse width is a sinusoidal function of the angular position of the pulse in a cycle. This is termed as sinusoidal PWM.

In sinusoidal Pulse Width Modulation, the gating signal is generated by comparing the sinusoidal reference wave with triangular carrier wave. The width of each pulse is varied in proportion to the amplitude of a sine wave evaluated at the center of the same pulse. The frequency of reference signal f_r , determines the inverter output frequency and its peak amplitude A_r controls the modulation index M which controls the rms output voltage[9].

2.4 SPACE VECTOR PWM

2.4.1 Introduction

The space vector PWM (SVM) method is an advanced, computation-intensive PWM method and is possibly the best among all the PWM techniques for variable-frequency drive applications. Because of its superior performance characteristics, it has been finding widespread application in recent year

Pulse Width Modulation technique is used to generate the required voltage or current to feed the motor or phase signals. This method is increasingly used for AC drives with the condition that the harmonic current is as small as possible and the maximum

output voltage is as large as possible. Generally, the PWM schemes generate the switching position patterns by comparing three-phase sinusoidal waveforms with a triangular carrier. In recent years, the space vector theory demonstrated some improvement for both the output crest voltage and the harmonic copper loss. The maximum output voltage based on the space vector theory is $2/3 = 1.155$ times as large as the conventional sinusoidal modulation. It enables to feed the motor with a higher voltage than the easier sub-oscillation modulation method. This modulator allows a higher torque at high speeds, and a higher efficiency. It also minimizes THD and switching loss. The controlled variables are motor voltage and motor frequency[16].

2.4.2 Inverter Switching States

To understand the SVM theory, the concept of a rotating space vector discussed in[16] is very important. For example, if three-phase sinusoidal and balanced voltages given by the equations

$$v_{as} = v_m \cos(\omega t) \quad (2.1)$$

$$v_{bs} = v_m \cos\left(\omega t - \frac{2\pi}{3}\right) \quad (2.2)$$

$$v_{cs} = v_m \cos\left(\omega t + \frac{2\pi}{3}\right) \quad (2.3)$$

are applied to a three-phase induction motor, it is shown that the space vector V with magnitude V_m rotates in circular orbit at angular velocity ω , where the direction of rotation depends on the phase sequence of the voltages[16].

When the instantaneous phase voltages are v_{as} , v_{bs} and v_{cs} then space-vector is defined as

$$v = 2/3(v_{as} + av_{bs} + a^2v_{cs}) \quad (2.4)$$

where $a = e^{j2\pi/3}$

From the equation (2.1) (2.2) (2.3) and (2.4) space-vector of voltage is simplified to

$$v = v_m e^{j\omega t} \quad (2.5)$$

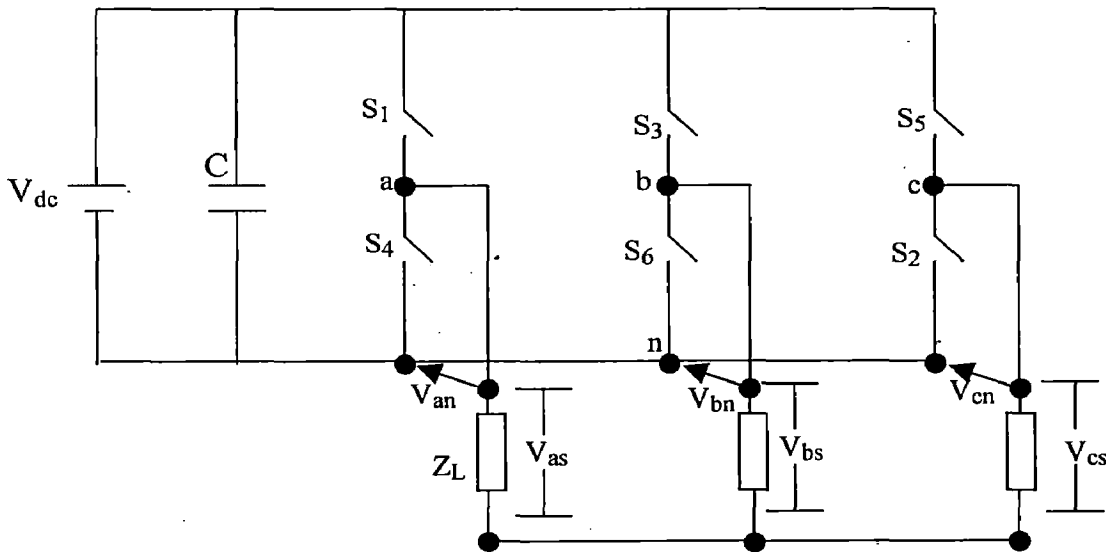


Fig 2.1 Switch model of a Three-phase Inverter

In the space vector PWM theory, the motor voltage vector is approximated by a combination of 8 switching states of three upper and three lower power switches that feed the three phase power inverter. The changeover switch model of a voltage source inverter is shown in Fig. 2.1. The state of the switches can be defined by the switching functions S_a , S_b and S_c . Their value is 0 when the corresponding phase is connected to the negative dc-voltage and 1 when it is connected to the positive dc-voltage. The phase voltage with respect to negative dc voltage can be defined as[12]

$$\begin{aligned} v_{an} &= S_a V_{dc} \\ v_{bn} &= S_b V_{dc} \\ v_{cn} &= S_c V_{dc} \end{aligned} \quad (2.6)$$

And line to voltage are:

$$\begin{aligned} v_{ab} &= v_{an} - v_{bn} \\ v_{bc} &= v_{bn} - v_{cn} \\ v_{ca} &= v_{cn} - v_{an} \end{aligned} \quad (2.7)$$

The sum of phase currents is zero as there is no zero sequence current. In a symmetric load also the sum of phase voltages is zero, $v_{as} + v_{bs} + v_{cs} = 0$. Because line-to-line voltages are also obtained from

$$\begin{aligned}v_{ab} &= v_{as} - v_{bs} \\v_{bc} &= v_{bs} - v_{cs} \\v_{ca} &= v_{cs} - v_{as}\end{aligned}\tag{2.8}$$

So the phase voltage can be obtained as

$$\begin{aligned}v_{as} &= \left(\frac{2}{3}\right)v_{an} - \left(\frac{1}{3}\right)(v_{bn} + v_{cn}) \\v_{bs} &= \left(\frac{2}{3}\right)v_{bn} - \left(\frac{1}{3}\right)(v_{cn} + v_{an}) \\v_{cs} &= \left(\frac{2}{3}\right)v_{cn} - \left(\frac{1}{3}\right)(v_{an} + v_{bn})\end{aligned}\tag{2.9}$$

Now the space vector of output voltage is

$$\begin{aligned}v &= 2/3(v_{as} + av_{bs} + a^2v_{cs}) \\ \text{Or } v &= 2/3(v_{an} + av_{bn} + a^2v_{cn}) \\ \text{Or } v &= 2/3V_{dc}(S_a + aS_b + a^2S_c)\end{aligned}\tag{2.10}$$

The inverter has six states when a voltage is applied to the motor and two states (7 and 8) when the motor is shorted through the upper and lower switches resulting in zero volts being applied to motor. It is useful to express these states as vectors. v_{1-8} express three voltages v_{as}, v_{bs}, v_{cs} that are spatially separated 120° apart as a space vector, v for each of the switching states 1-8. The six vectors including of zero voltage vectors can be expressed geometrically as shown in Fig 2.2. The eight combinations are the derived output line-to-line and phase voltages in terms of DC supply voltage V_{dc} according to equations (2.7) and (2.9)

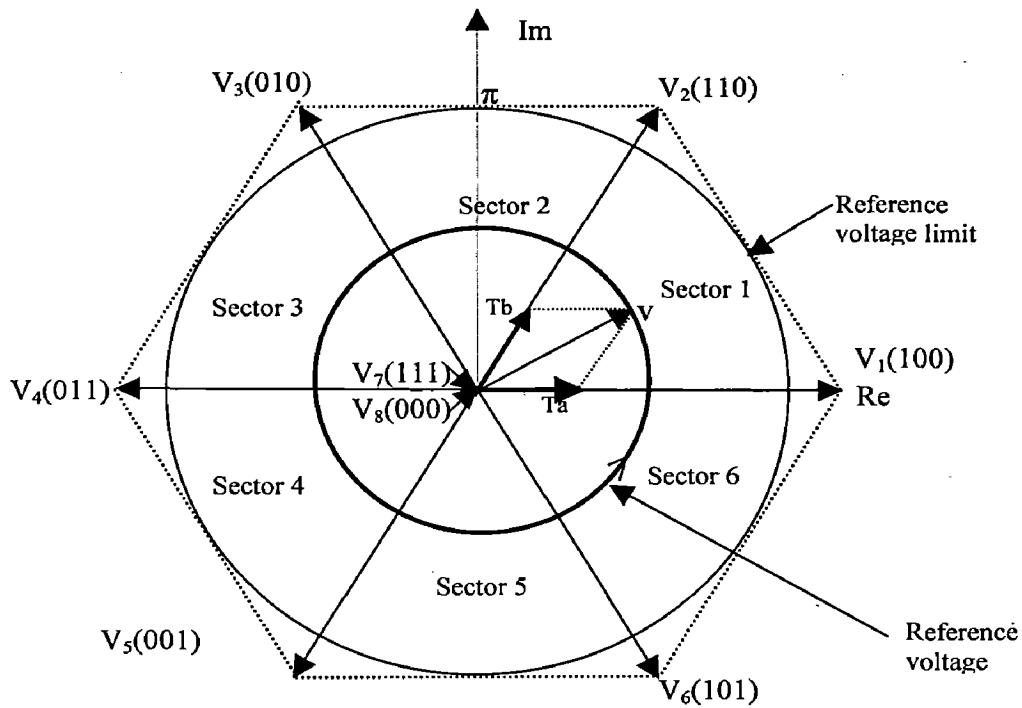


Fig 2.2 Space Vector Diagram

Table 2.1 gives a summary of the switching states and the corresponding phase-to-neutral voltage of an isolated neutral machine. Consider, for example, state 1, when S_1 , S_6 and S_2 are closed. In this state, phase a is connected to the positive bus and phases b and c are connected to the negative bus. The simple circuit solution indicates

State	On Devices	V_{as}	V_{bs}	V_{cs}	V_{ab}	V_{bc}	V_{ca}	Space Voltage Vector
1	$S_1S_6S_2$	$2/3V_{dc}$	$-1/3 V_{dc}$	$-1/3 V_{dc}$	V_{dc}	0	$-V_{dc}$	$V_1(100)$
2	$S_1S_3S_2$	$1/3 V_{dc}$	$1/3 V_{dc}$	$-2/3V_{dc}$	0	V_{dc}	$-V_{dc}$	$V_2(110)$
3	$S_4S_3S_2$	$-1/3 V_{dc}$	$2/3V_{dc}$	$-1/3 V_{dc}$	$-V_{dc}$	V_{dc}	0	$V_3(010)$
4	$S_4S_3S_5$	$-2/3 V_{dc}$	$1/3 V_{dc}$	$1/3 V_{dc}$	$-V_{dc}$	0	V_{dc}	$V_4(011)$
5	$S_4S_6S_5$	$-1/3 V_{dc}$	$-1/3 V_{dc}$	$2/3V_{dc}$	0	$-V_{dc}$	V_{dc}	$V_5(001)$
6	$S_1S_6S_5$	$1/3 V_{dc}$	$-2/3V_{dc}$	$1/3 V_{dc}$	V_{dc}	$-V_{dc}$	0	$V_6(101)$
7	$S_1S_3S_5$	0	0	0	0	0	0	$V_7(111)$
8	$S_4S_6S_2$	0	0	0	0	0	0	$V_8(000)$

Table 2.1 Summary of Inverter Switching States

that $v_{as} = 2/3V_{dc}$, $v_{bs} = -1/3V_{dc}$ and $v_{cs} = -1/3V_{dc}$. The sets of phase voltages for each switching state can be combined with the help of Equation (2.4) to derive the corresponding space vectors.

The eight combinations and the derived output line-to-line and phase voltages are shown in Table 2.1.

The graphical derivation of $V_1(100)$ in Fig 2.3. indicates that the vector has a magnitude of $2/3V_{dc}$ and is aligned in the horizontal direction as shown. In the same way, all six vectors and two zero vectors are derived.

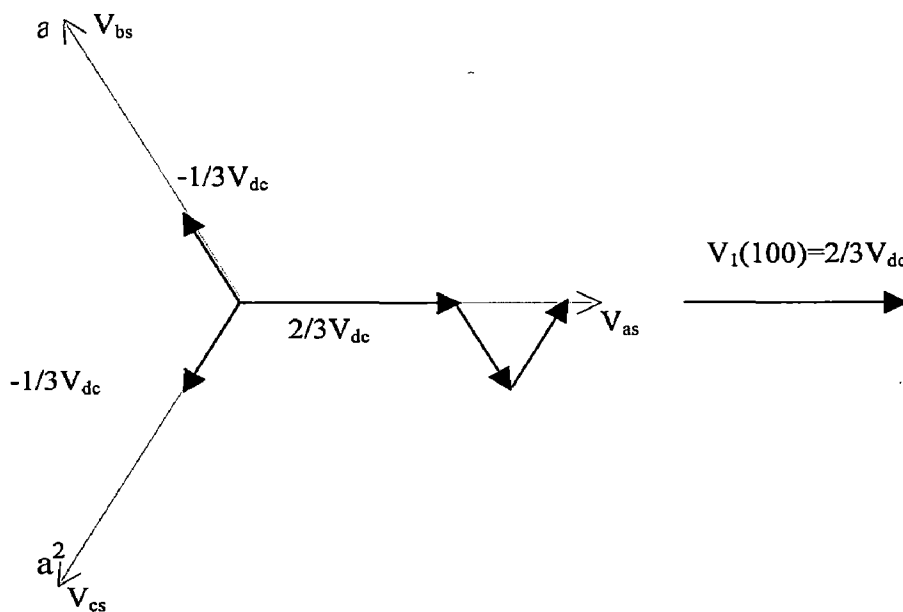


Fig 2.3 Construction of inverter space vector $V_1(100)$

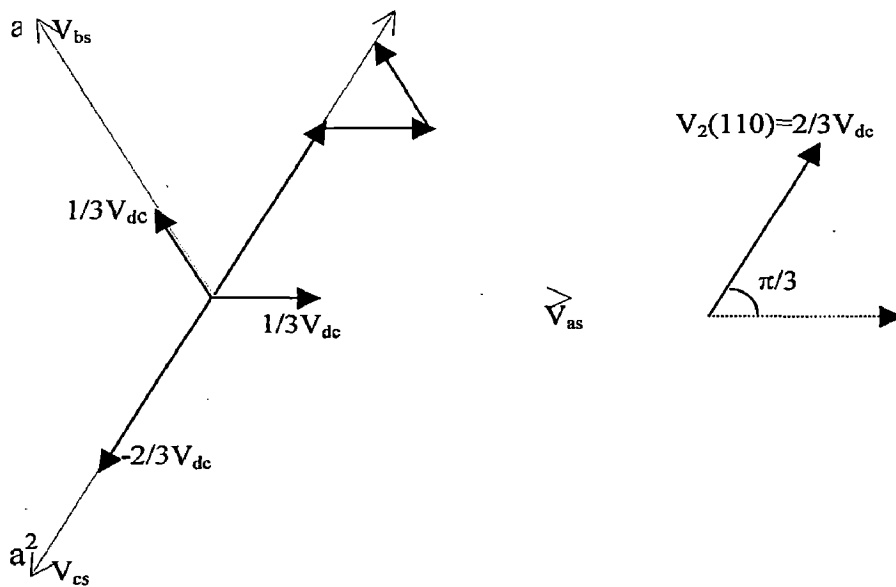


Fig 2.4 Construction of inverter space vector $V_2(110)$

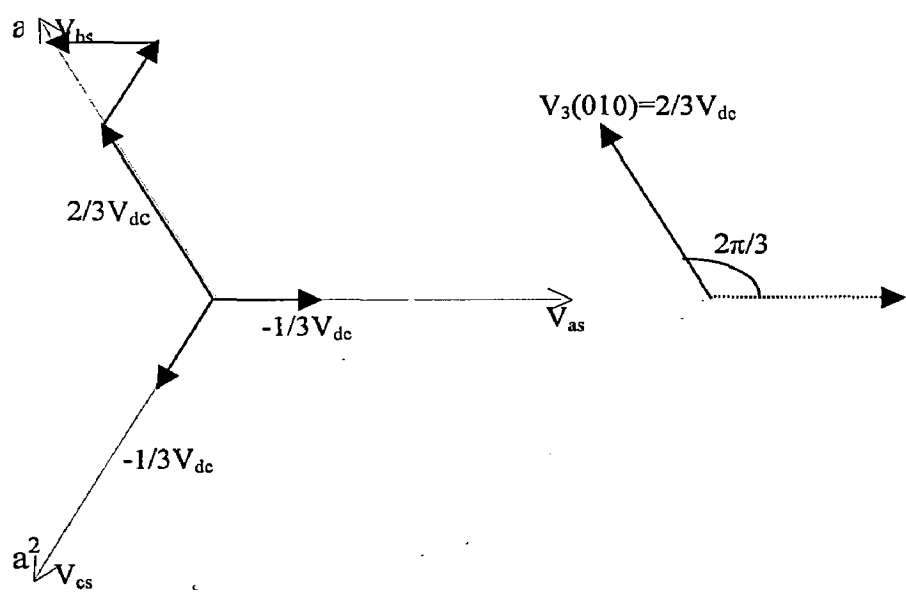


Fig 2.5 Construction of inverter space vector $V_3(010)$

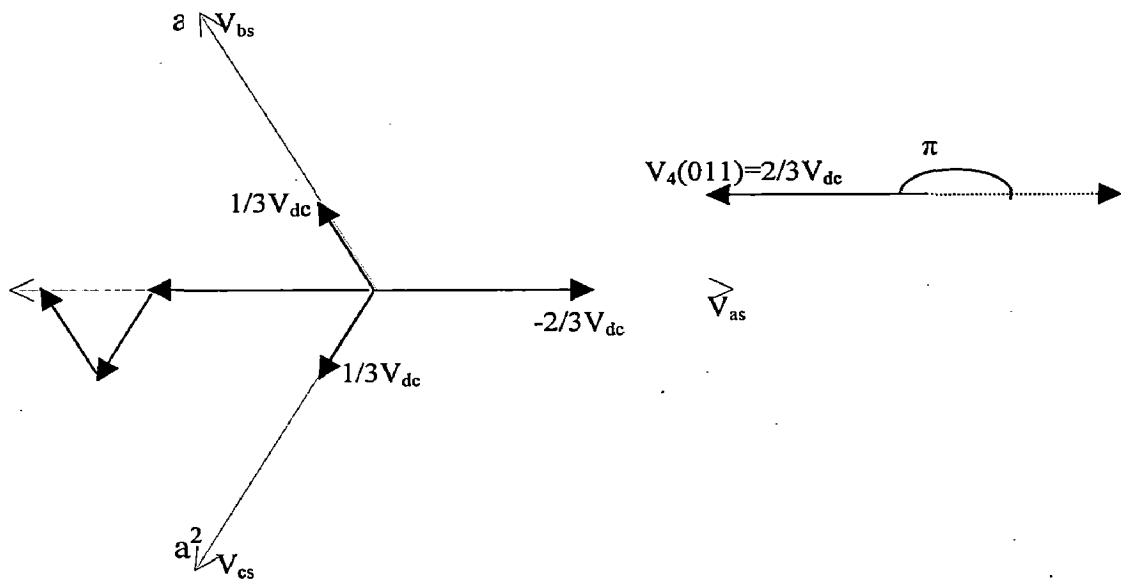


Fig 2.6 Construction of inverter space vector $V_4(011)$

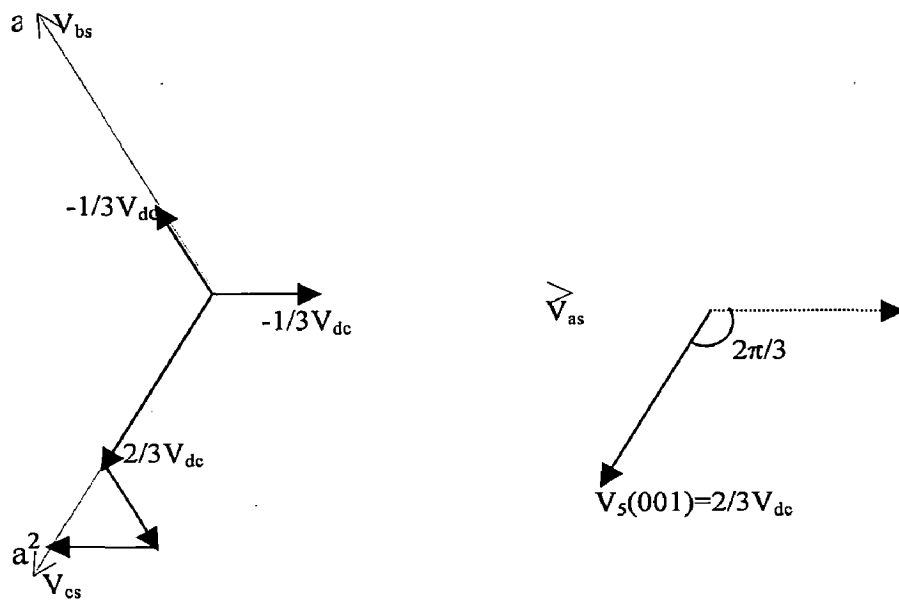


Fig 2.7 Construction of inverter space vector $V_5(001)$

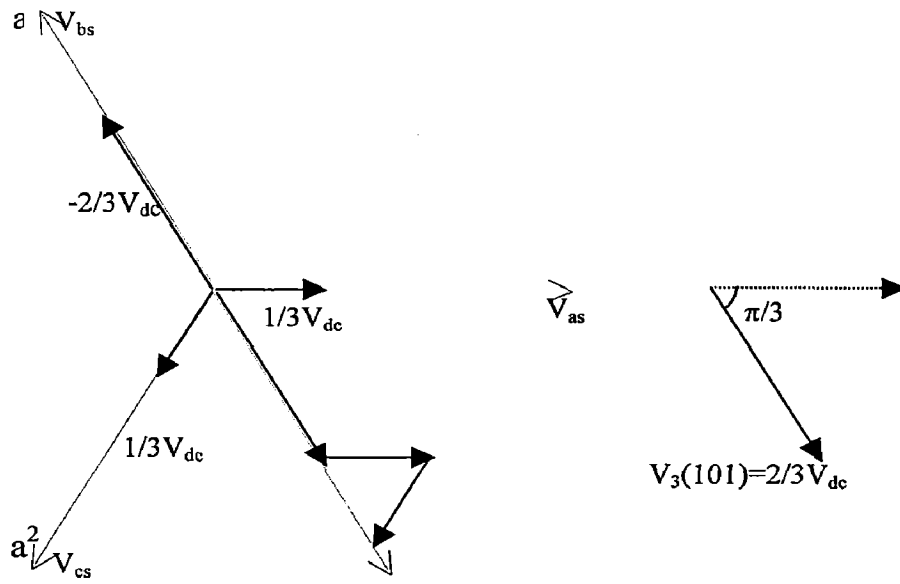


Fig 2.8 Construction of inverter space vector $V_6(101)$

CHAPTER – 3

MATHEMATICAL MODEL OF AN INDUCTION MOTOR DRIVE

This chapter presents the development of generalized equations describing the behavior of the cage induction motor drive based on the coupled circuit approach. The system has been analyzed in a stationary reference frame. With the help of d-q transformation of variables, basic equations for induction motor, is developed in per unit system. The mathematical model of developed has been used in present study for analysis purpose of the drive under space vector modulation technique.

The steps involved in determining the mathematical model of an electrical rotating machine are as follow;

1. Various phases or winding of machine are identified as coils having certain resistance, self-induction and mutual inductions. The equations are written for balance voltage. The equation contain
 - (a) Ohmic drop in the resistance of coil.
 - (b) Self induction voltage in the coil.
 - (c) Voltage induced in the coil due to mutual coupling.
 - (d) Voltage induced due to rotation.
2. Since there is relative motion between stator and rotor, coil inductances are assumed as a function of rotor position. Thus, the linear transformation is derived to convert the impedance matrix to certain coefficient.

3.1 DEVELOPMENT OF MATHEMATICAL MODEL OF THE INDUCTION MOTOR

The generalized equations describing the behavior of an induction motor under steady state and transient condition are established. For the analysis of induction motor following assumptions are made:

1. The motor magnetic circuit is considering linear and saturation is neglected.
2. Core, friction, windage and stray load losses are not consider in the analysis.
3. The neural of motor is not grounded; consequently, the current and flux linkage of coordinate zero can be neglected.
4. The switches are assumed ideal.

The ideal three-phase induction motor, can be schematically represented in fig. 3.1, is regarded as a group of linear coupled circuits. Distributed stator and rotor winding have been shown by concentrated coils. The connections and current conventions for the stator phases are shown in fig. 3.2 and the angular relationship of various axes is shown in fig. 3.3. The axis of a rotor phase is displayed by an angle θ_r from the axis of the corresponding stator phase. As the rotor rotates, the angle θ_r varies with time and is given by

$$p\theta_r = \omega_r \quad (3.1)$$

Where, ω_r is angular speed of rotor (in elect. rad./sec.). If ω_e is the synchronous speed (in elect. rad./sec.) then slip is given by

$$s = \left(\frac{(\omega_e - \omega_r)}{\omega_e} \right) \quad (3.2)$$

The d-q reference frame is considered to be rotating with arbitrary speed ω with respect to the stator. Thus, considering the q-axis to be consider with phase-a axis of the stator at time t=0, it will advance by an angle θ such that

$$p\theta = \omega \quad (3.3)$$

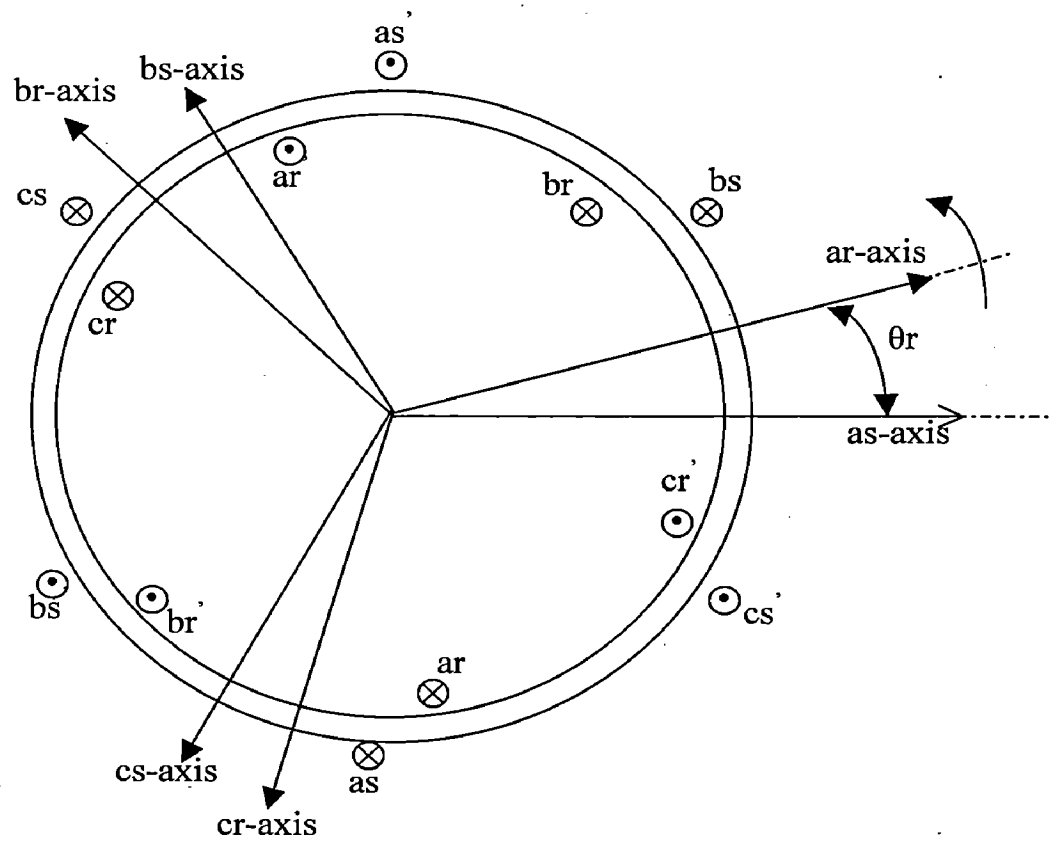


Fig 3.1 Idealized three phase Induction motor

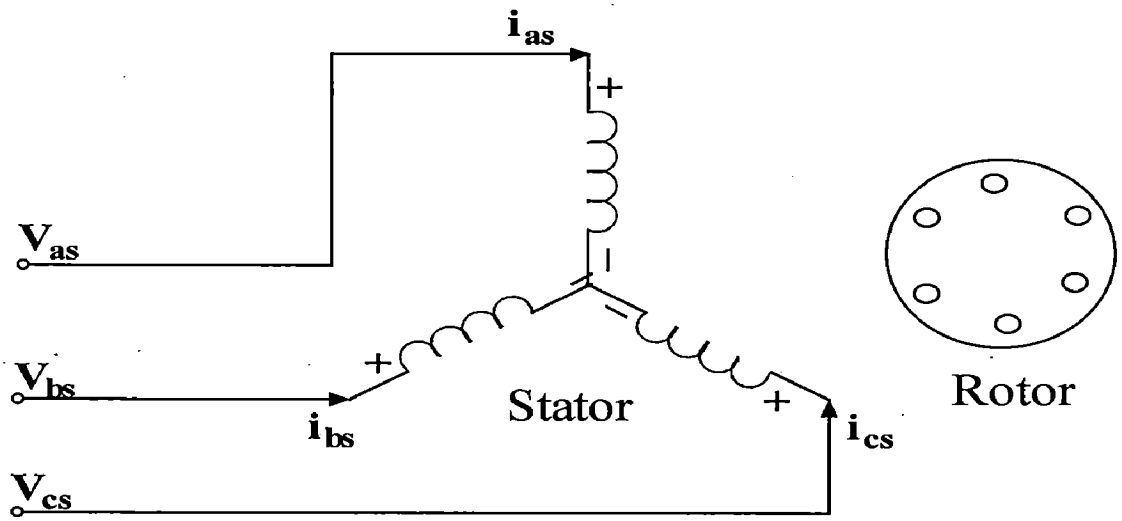


Fig 3.2 Connections and current conventions for a 3-phase Squirrel cage Induction motor

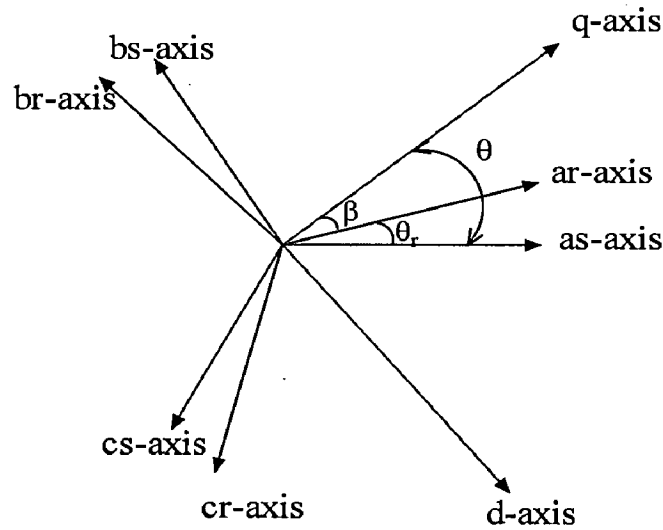


Fig. 3.3 Axes of a 3-phase symmetrical Induction motor

The angle β between the d-axis and rotor phase-a axis is then given by

$$\beta = \theta - \theta_r \quad (3.4)$$

The voltage-current relations for the stator and rotor windings are given by the following expression[11]:

For stator

$$v_{as} = i_{as} R_s + p\lambda_{as} \quad (3.5)$$

$$v_{bs} = i_{bs} R_s + p\lambda_{bs} \quad (3.6)$$

$$v_{cs} = i_{cs} R_s + p\lambda_{cs} \quad (3.7)$$

Where $p\lambda_{as}$, $p\lambda_{bs}$ and $p\lambda_{cs}$ are induced emf in stator phase a, b and c respectively.

For rotor

$$v_{ar} = i_{ar} R_r + p\lambda_{ar} \quad (3.8)$$

$$v_{br} = i_{br} R_r + p\lambda_{br} \quad (3.9)$$

$$v_{cr} = i_{cr} R_r + p\lambda_{cr} \quad (3.10)$$

Where $p\lambda_{ar}$, $p\lambda_{br}$ and $p\lambda_{cr}$ are induced emf in rotor phase a, b and c respectively.

For a magnetically linear system, the flux linkages may be expressed as

$$\begin{bmatrix} \lambda_{abcs} \\ \lambda_{abcr} \end{bmatrix} = \begin{bmatrix} L_s & L_{sr} \\ (L_{sr})^T & L_r \end{bmatrix} \begin{bmatrix} i_{abcs} \\ i_{abcr} \end{bmatrix} \quad (3.11)$$

Where

$$\begin{aligned} (\lambda_{abcs})^T &= [\lambda_{as} \quad \lambda_{bs} \quad \lambda_{cs}] \\ (\lambda_{abcr})^T &= [\lambda_{ar} \quad \lambda_{br} \quad \lambda_{cr}] \\ (i_{abcs})^T &= [i_{as} \quad i_{bs} \quad i_{cs}] \\ (i_{abcr})^T &= [i_{ar} \quad i_{br} \quad i_{cr}] \end{aligned} \quad (3.12)$$

Self-induction of stator and rotor phase, mutual inductions between stator phases and mutual inductions between rotor phases are constant because of smooth rotor construction, but the mutual inductions between a stator phase and a rotor phase depends

on the position of rotor, the instantaneous value being proportional to cosine of the angle between stator and rotor axes at that instant[11].

So the winding induction are derived as

$$L_s = \begin{bmatrix} L_{ls} + L_{ms} & -1/2L_{ms} & -1/2L_{ms} \\ -1/2L_{ms} & L_{ls} + L_{ms} & -1/2L_{ms} \\ -1/2L_{ms} & -1/2L_{ms} & L_{ls} + L_{ms} \end{bmatrix} \quad (3.15)$$

$$L_r = \begin{bmatrix} L_{lr} + L_{mr} & -1/2L_{mr} & -1/2L_{mr} \\ -1/2L_{mr} & L_{lr} + L_{mr} & -1/2L_{mr} \\ -1/2L_{mr} & -1/2L_{mr} & L_{lr} + L_{mr} \end{bmatrix} \quad (3.16)$$

$$L_{sr} = L_{sr} \begin{bmatrix} \cos(\theta_r) & \cos(\theta_r + 2\pi/3) & \cos(\theta_r - 2\pi/3) \\ \cos(\theta_r - 2\pi/3) & \cos(\theta_r) & \cos(\theta_r + 2\pi/3) \\ \cos(\theta_r + 2\pi/3) & \cos(\theta_r - 2\pi/3) & \cos(\theta_r) \end{bmatrix} \quad (3.17)$$

In the above inductances equations, L_{ls} and L_{ms} are respectively, the leakage and magnetizing inductances of stator winding; L_{lr} and L_{mr} are for the rotor windings. The inductance L_{ls} is the amplitude of the mutual inductance between stator and rotor windings.

When expressing the voltage equations in machine variable form, it is convenient to refer all rotor variables to stator winding by appropriate tern ratio ($n=N_s/N_r$)

$$\begin{aligned} i'_{abcr} &= (1/n)i_{abcr} \\ v'_{abcr} &= nv_{abcr} \\ \lambda'_{abcr} &= n\lambda_{abcr} \end{aligned} \quad (3.18)$$

The magnetizing and mutual inductances are associated with the same magnetic path: therefore

$$L_{ms} = nL_{sr} \quad \text{and} \quad L_{mr} = (1/n)^2 L_{ms}$$

Thus, we will define

$$L'_{sr} = nL_{sr} \quad \text{or}$$

$$L'_{sr} = L_{ms} \begin{bmatrix} \cos(\theta_r) & \cos(\theta_r + 2\pi/3) & \cos(\theta_r - 2\pi/3) \\ \cos(\theta_r - 2\pi/3) & \cos(\theta_r) & \cos(\theta_r + 2\pi/3) \\ \cos(\theta_r + 2\pi/3) & \cos(\theta_r - 2\pi/3) & \cos(\theta_r) \end{bmatrix} \quad (3.19)$$

And if let

$$L'_r = n^2 L_r \text{ Then}$$

$$L'_r = \begin{bmatrix} L'_{lr} + L_{ms} & -1/2L_{ms} & -1/2L_{ms} \\ -1/2L_{ms} & L'_{lr} + L_{ms} & -1/2L_{ms} \\ -1/2L_{ms} & -1/2L_{ms} & L'_{lr} + L_{ms} \end{bmatrix} \quad (3.20)$$

Where

$$L'_{lr} = n^2 L_{lr}$$

The flux linkage may now be expressed as

$$\begin{bmatrix} \lambda_{abcs} \\ \lambda'_{abcr} \end{bmatrix} = \begin{bmatrix} L_s & L'_{sr} \\ (L'_{sr})^T & L'_r \end{bmatrix} \begin{bmatrix} i_{abcs} \\ i'_{abcr} \end{bmatrix} \quad (3.21)$$

The voltage equations expressed in terms of machine variables referred to the stator windings may now be written as

$$\begin{bmatrix} v_{abcs} \\ v'_{abcr} \end{bmatrix} = \begin{bmatrix} r_s + pL_s & pL'_{sr} \\ p(L'_{sr})^T & r'_r + pL'_r \end{bmatrix} \begin{bmatrix} i_{abcs} \\ i'_{abcr} \end{bmatrix} \quad (3.22)$$

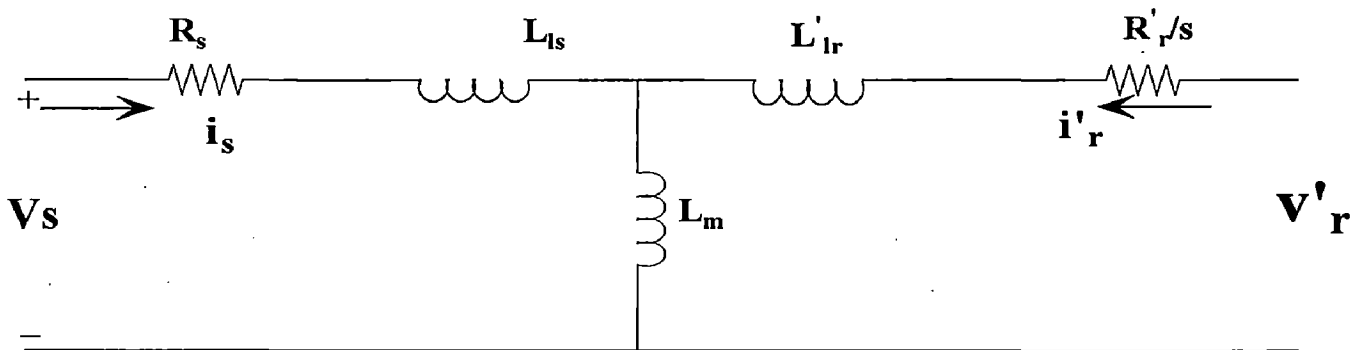


Fig. 3.4 Conventional per-phase equivalent circuit for a 3-phase, symmetrical Induction motor

3.2 D-Q MODEL OF INDUCTION MOTOR

After solving the equations (3.5) to (3.22), gives a set of differential equation of voltages and flux linkage, which are non-linear due to time varying nature of the coefficients. These equations can, however, be converted to a set of linear equations by adopting d-q transformation. By doing so the time varying coefficient are eliminated, and the variables and parameters are expressed in mutually decoupled direct and quadrature axes. The d-q equation of an induction motor can be expressed in arbitrary reference frame (i.e. stationary, rotating with rotor or synchronously rotating reference frame.). The use of a reference frame that rotates at synchronous speed provides advantages that with sinusoidal excitation the variable appear as dc quantities in steady state conditions[22].

3.3 MOTOR EQUATIONS IN ARBITRARYT REFERENCE FRAME

The voltage equation in arbitrary reference frame (d-q model) can be written as

$$\begin{aligned} v_{qdos} &= r_s i_{qdos} + \omega \lambda_{dqs} + p \lambda_{qdos} \\ v'_{qdor} &= r'_r i'_{qdor} + (\omega - \omega_r) \lambda'_{dqr} + p \lambda'_{qdor} \end{aligned} \quad (3.23)$$

The set of equations is complete once the expressions for flux linkages are determined. The flux linkage equations for a magnetically linear system can be written as

$$\begin{bmatrix} \lambda_{qdos} \\ \lambda'_{qdor} \end{bmatrix} = \begin{bmatrix} K_s L_s (K_s)^{-1} & K_s L'_{sr} (K_r)^{-1} \\ (K_r (L'_{sr})^T (K_s))^{-1} & K_r L'_r (K_r)^{-1} \end{bmatrix} \begin{bmatrix} i_{qdos} \\ i'_{qdor} \end{bmatrix} \quad (3.24)$$

Where

$$\begin{aligned} (\lambda_{qds})^T &= \begin{bmatrix} \lambda_{ds} & -\lambda_{qs} & 0 \end{bmatrix} \\ (\lambda'_{qdr})^T &= \begin{bmatrix} \lambda'_{dr} & -\lambda'_{qr} & 0 \end{bmatrix} \end{aligned}$$

And K_s is a transformation matrix, which transform the 3-phase variable of stationary circuit elements into arbitrary reference frame.

$$K_s = \frac{2}{3} \begin{bmatrix} \cos(\theta) & \cos(\theta - 2\pi/3) & \cos(\theta + 2\pi/3) \\ \sin(\theta) & \sin(\theta - 2\pi/3) & \sin(\theta + 2\pi/3) \\ 1/2 & 1/2 & 1/2 \end{bmatrix} \quad (3.25)$$

Similarly K_r is a transformation matrix, which transforms the 3-phase variable of rotating circuit elements into arbitrary reference frame

$$K_s = \frac{2}{3} \begin{bmatrix} \cos(\beta) & \cos(\beta - 2\pi/3) & \cos(\beta + 2\pi/3) \\ \sin(\beta) & \sin(\beta - 2\pi/3) & \sin(\beta + 2\pi/3) \\ 1/2 & 1/2 & 1/2 \end{bmatrix} \quad (3.26)$$

The voltage equations after written in expanded form. From (3.24) we obtain

$$v_{qs} = R_s i_{qs} + \omega \lambda_{ds} + p \lambda_{qs} \quad (3.27)$$

$$v_{ds} = R_s i_{ds} - \omega \lambda_{qs} + p \lambda_{ds} \quad (3.28)$$

$$v'_{qr} = R'_r i'_{qr} + (\omega - \omega_r) \lambda'_{dr} + p \lambda'_{qr} \quad (3.29)$$

$$v'_{dr} = R'_r i'_{dr} - (\omega - \omega_r) \lambda'_{qr} + p \lambda'_{dr} \quad (3.30)$$

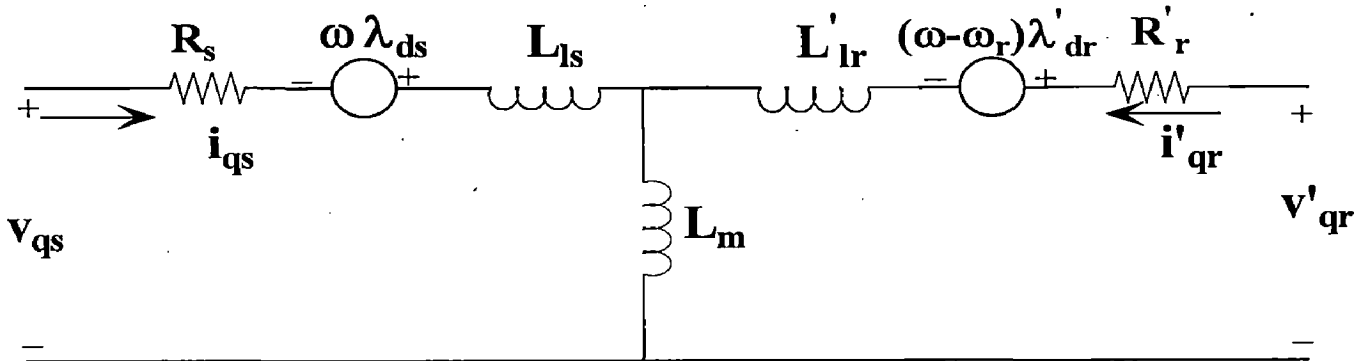


fig. (a): q-axis circuit

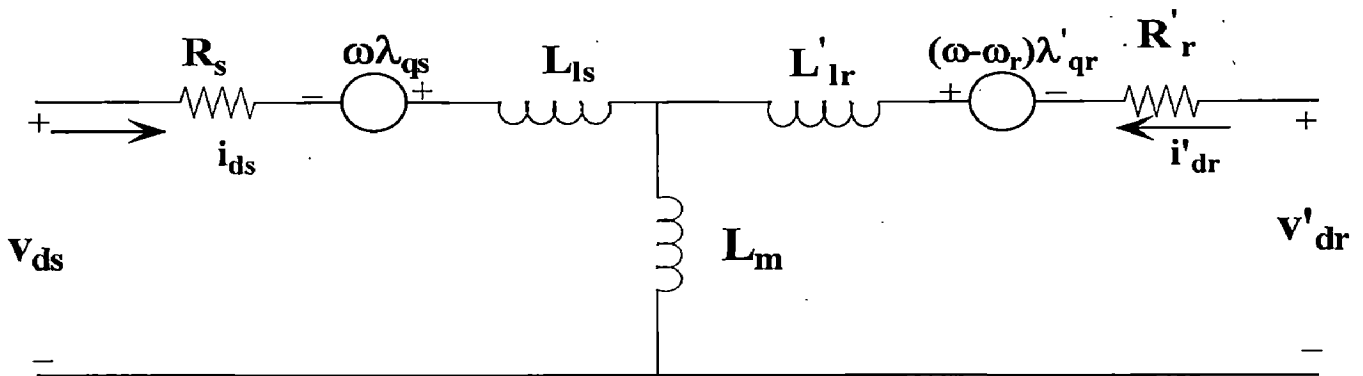


fig. (b): d-axis circuit

Fig. 3.5 Arbitrary reference frame equivalent circuit for a 3-phase, symmetrical Induction motor

Substituting (3.15), (3.19), (3.20), (3.25) and (3.26) into (3.24) yields the expressions for the flux linkages. In expanded form we have

$$\lambda_{qs} = L_{ls} i_{qs} + L_m (i_{qs} + i'_{qr}) \quad (3.31)$$

$$\lambda_{ds} = L_{ls} i_{ds} + L_m (i_{ds} + i'_{dr}) \quad (3.32)$$

$$\lambda'_{qr} = L'_{lr} i'_{qr} + L_m (i_{qs} + i'_{qr}) \quad (3.33)$$

$$\lambda'_{dr} = L'_{lr} i'_{dr} + L_m (i_{ds} + i'_{dr}) \quad (3.34)$$

In addition, electromagnetic torque of induction motor can be calculated as

$$T_e = \left(\frac{3}{2}\right) \left(\frac{P}{2}\right) (\lambda_{ds} i_{qs} - \lambda_{qs} i_{ds}) \quad (3.35)$$

Because machine parameter is taken in per unit so it is convenient to express the voltage and flux linkage in terms of reactance rather than inductances. Hence, (3.27 to 3.30) are written as

$$v_{qs} = R_s i_{qs} + \frac{\omega}{\omega_b} \psi_{ds} + \frac{1}{\omega_b} p \psi_{qs} \quad (3.36)$$

$$v_{ds} = R_s i_{ds} - \frac{\omega}{\omega_b} \psi_{qs} + \frac{1}{\omega_b} p \psi_{ds} \quad (3.37)$$

$$v'_{qr} = R'_r i'_{qr} + \left(\frac{\omega - \omega_r}{\omega_b}\right) \psi'_{dr} + \frac{1}{\omega_b} p \psi'_{qr} \quad (3.38)$$

$$v'_{dr} = R'_r i'_{dr} - \left(\frac{\omega - \omega_r}{\omega_b}\right) \psi'_{qr} + \frac{1}{\omega_b} p \psi'_{dr} \quad (3.39)$$

Where ω_b is the base electrical angular velocity used to calculate the inductive reactance.

Flux linkages (3.31 to 3.34) now become flux linkage per second with units of volts.

$$\psi_{qs} = X_{ls} i_{qs} + X_m (i_{qs} + i'_{qr}) \quad (3.40)$$

$$\psi_{ds} = X_{ls} i_{ds} + X_m (i_{ds} + i'_{dr}) \quad (3.41)$$

$$\psi'_{qr} = X'_{lr} i'_{qr} + X_m (i_{qs} + i'_{qr}) \quad (3.42)$$

$$\psi'_{dr} = X'_{lr} i'_{dr} + X_m (i_{ds} + i'_{dr}) \quad (3.43)$$

And electromagnetic torque of induction motor

$$T_e = \left(\frac{3}{2}\right) \left(\frac{P}{2}\right) \left(\frac{1}{\omega_b}\right) (\psi_{ds} i_{qs} - \psi_{qs} i_{ds}) \quad (3.44)$$

3.4 MOTOR EQUATIONS IN STATIONARY REFERENCE FRAME

When induction motors are controlled through *Direct Torque Control schemes*, control computation is often done in the *stationary reference frame*. So the induction motor dynamic model in stationary reference frame can be calculated from equation (3.36) to (3.43) where $\omega = 0$. Since the rotor is short-circuited so $v'_{qr} = v'_{dr} = 0$. After simplified

$$\psi_{qs} = \left(\frac{\omega_b}{p}\right) \left(v_{qs} + \left(\frac{R_s}{X_{ls}}\right) (\psi_{mq} - \psi_{qs}) \right) \quad (3.45)$$

$$\psi_{ds} = \left(\frac{\omega_b}{p}\right) \left(v_{ds} + \left(\frac{R_s}{X_{ls}}\right) (\psi_{md} - \psi_{ds}) \right) \quad (3.46)$$

$$\psi'_{qr} = \left(\frac{\omega_b}{p}\right) \left(\left(\frac{\omega_r}{\omega_b}\right) \psi'_{dr} + \left(\frac{R_s}{X_{lr}}\right) (\psi_{mq} - \psi'_{qr}) \right) \quad (3.47)$$

$$\psi'_{dr} = \left(\frac{\omega_b}{p}\right) \left(\left(\frac{\omega_r}{\omega_b}\right) \psi'_{qr} + \left(\frac{R_s}{X_{lr}}\right) (\psi_{md} - \psi'_{dr}) \right) \quad (3.48)$$

And electromagnetic torque is given as

$$T_e = \left(\frac{3}{2}\right) \left(\frac{P}{2}\right) \left(\frac{1}{\omega_b}\right) (\psi_{ds} i_{qs} - \psi_{qs} i_{ds}) \quad (3.49)$$

Where

$$\psi_{mq} = X_{aq} \left(\frac{\psi_{qs}}{X_{ls}} + \frac{\psi'_{qr}}{X_{lr}} \right) \quad (3.50)$$

$$\psi_{md} = X_{aq} \left(\frac{\psi_{ds}}{X_{ls}} + \frac{\psi'_{dr}}{X_{lr}} \right) \quad (3.51)$$

$$X_{aq} = \left(\frac{1}{X_{ls}} + \frac{1}{X_{lr}} + \frac{1}{X_m} \right)^{-1}$$

$$i_{qs} = \frac{1}{X_{ls}} (\psi_{qs} - \psi_{mq}) \quad (3.52)$$

$$i_{ds} = \frac{1}{X_{ls}} (\psi_{ds} - \psi_{md}) \quad (3.53)$$

$$i'_{qr} = \frac{1}{X_{lr}} (\psi'_{qr} - \psi_{mq}) \quad (3.54)$$

$$i'_{dr} = \frac{1}{X_{lr}} (\psi'_{dr} - \psi_{md}) \quad (3.55)$$

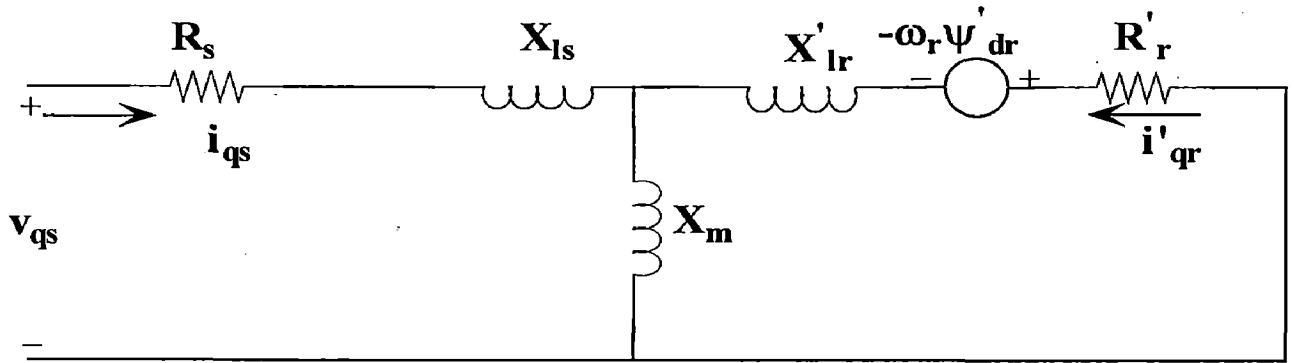


fig. (a): q-axis circuit

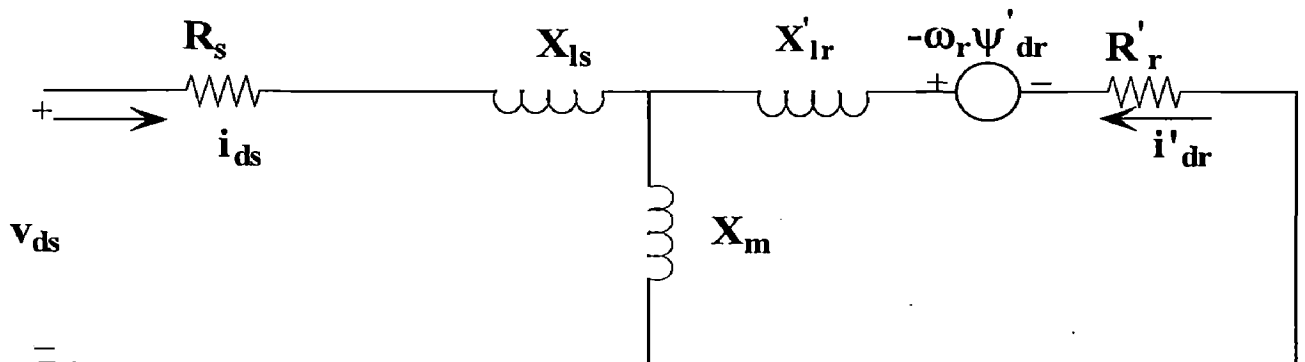


fig. (b): d-axis circuit

Fig. 3.6 Stationary reference-frame equivalent circuit for a 3-phase, symmetrical squirrel-cage Induction motor

3.5 PER UNIT SYSTEM

When per unit system form is chosen to express various quantizes of a machine system, two distinct advantage results. One is that machine parameters of system lie in a reasonably narrow numerical range. Their correctness or otherwise can therefore be established through a rapid check. The narrow range also facilitates simulation of the machine system on digital computer. The other is that arbitrary numerical factor, which may appear in the ordinary equation in d-q model transformation, disappear in per unit form, leading to simple equation[11].

For per unit conversion various variable and parameters are expresses in terms of their base value. The base value are define as

Base voltage

$$V_{\text{base}} = \text{peak value of rated phase voltage of the induction motor in volts } (V_{\text{sm}})$$

Base current

$$I_{\text{base}} = \text{peak value of rated phase current of the induction motor in Amps } (I_{\text{sm}})$$

Therefore, base power and base impedance can be calculated as

Base power

$$\begin{aligned} P_{\text{base}} &= 3 * V_{\text{rms}} * I_{\text{rms}} \\ &= 3 * (V_{\text{sm}} / \sqrt{2} * I_{\text{sm}} / \sqrt{2}) \\ &= (3/2)(V_{\text{sm}} * I_{\text{sm}}) \end{aligned} \quad (3.56)$$

Base impedance

$$Z_{\text{base}} = V_{\text{base}} / I_{\text{base}} \text{ (in ohm)} \quad (3.57)$$

Base electrical speed

$$\omega_{\text{base}} = 2 * \pi * f \text{ (in elect. radians/ sec.)}, \text{ where } f \text{ is the rated supply frequency of the motor.}$$

Base torque

$$T_{\text{base}} = \frac{P_{\text{base}}}{(2/ P)\omega_{\text{base}}} \text{ (N-M)} \quad (3.58)$$

So the electromagnetic torque (in p.u.) can be calculated as

$$T_e = (\psi_{ds} i_{qs} - \psi_{qs} i_{ds}) \quad (3.59a)$$

Torque balance equation in p.u. of the drive is given below

$$T_e = T_L + 2Hp(\omega_r / \omega_{base}) \quad (3.59b)$$

Where T_L is p.u. torque, ω_r is rotor speed and H is the inertia constant of the drive in seconds.

If J is the inertia of the rotor in kg-m² then H can be calculated as

$$H = \left(\frac{1}{2}\right) \left(\frac{2}{P}\right) \left(\frac{J \omega_{base}}{P_{base}}\right) \quad (3.60)$$

Using the p.u. quantities, we can describe a dynamic model of squirrel cage induction motor drive. The p.u. equations have been used in present work to analyze the behaviour of the drive in traction application. The model developed can be used to predict the dominant feature of the drive under steady state and transient conditions. The model neglects hysteresis and eddy current losses.

CHAPTER: 4

DIRECT TORQUE CONTROL

There are many different ways to drive an induction motor. The main differences between them are the motor's performance and cost in its real implementation.

4.1 SCALAR CONTROL

Despite the fact that "voltage /frequency" (v/f) is the simplest controller, it is the most widespread, being in the majority of the industrial applications. It is known as a scalar control and acts imposing a constant relation between voltage and frequency. The structure is very simple. As in scalar control, due to the fact that the stator flux and the torque are not directly control, it doesn't provide a good accuracy in both speed and torque responses.

4.2 VECTOR CONTROL

In these types of controllers, there are control loop for controlling both the torque and the flux. The most widespread controller is the ones that use vector transform such as 'Park '. Its accuracy can reach values such as 0.5 % regarding the speed and 2% regarding the torque, even in stand still.

The main disadvantages are the huge computational capability required and the compulsory good identification of motor parameter.

4.3 DIRECT TORQUE CONTROL

In Direct Torque Control it is possible to control directly the stator flux and torque by selecting the approximate inverter state.

Its main feature are as follows

- Direct Torque Control and Direct stator Flux Control.
- Indirect control of stator current and voltages.
- Approximated sinusoidal stator fluxes and stator currents.

- High dynamic performance even at locked rotor.

This method presents the following advantage:

- Absence of co-ordinate transforms.
- Absence of voltage modulator block, as well as other controller such as pid controller for flux and torque.
- Minimal torque response time, even better than the vector controller

Although, some disadvantages are present:

- Possible problems during starting.
- Requirement of torque and flux estimators, implying the consequent parameters identification.
- Inherent torque and flux ripples.

4.3.1 Introduction

This method uses feedback control of torque and stator flux, which are computed from the measured stator voltage and current. The method uses a stator reference model of induction motor for its implementation, thereby avoiding the trigonometric operation in the coordinate transformation of the synchronous reference. This is the key advantages of the control scheme. The scheme uses stator flux-linkage control. This reduces the dependence of the scheme on many motor parameters, thus making it a robust scheme in the flux weakening region. The scheme depends only on stator resistance and on no other parameters. For its flux and torque control, this control scheme requires the position of the flux phasor, which is difficult to obtain in low and zero speeds from measured voltages and currents by using a torque processor. At such low speeds, these signals are very small, making scaling and accuracy problematic; also, the stator resistance variations introduce significant error in the flux-phasor computation. Invariably the low-speed suffers with the scheme without stator resistance compensation [17].

4.3.2 Implementation Scheme

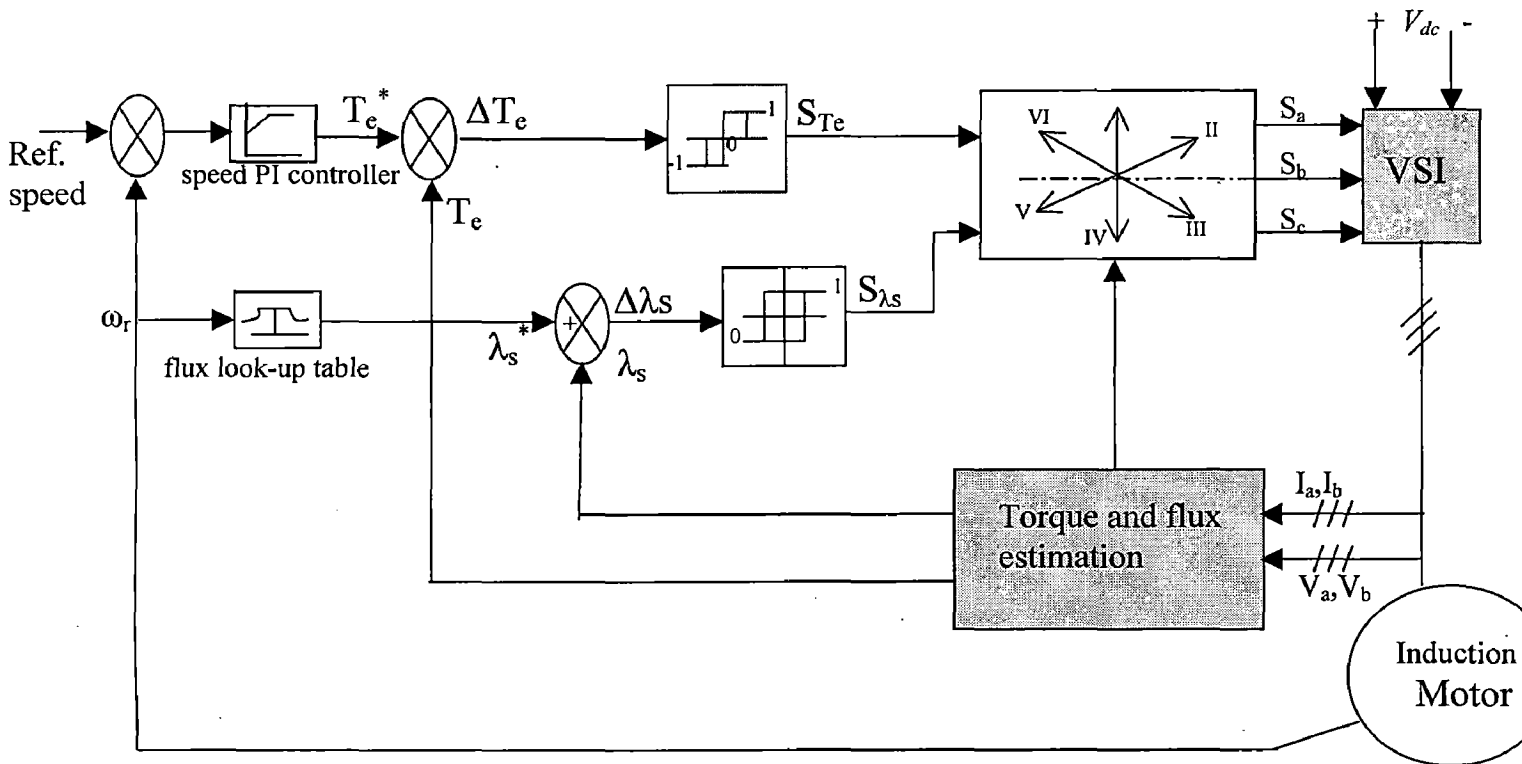


Fig. 4.1: Block diagram of DTC of Induction motor

The implementation of the scheme requires flux linkage and torque computation, plus generation of switching states through a feedback control of the torque and flux directly without inner current loop as shown in fig 4.1[12].

The stator q and d axes flux linkage (in stator reference frame) are

$$\begin{aligned}\lambda_{qs} &= \int (V_{qs} - R_s i_{qs}) dt \\ \lambda_{ds} &= \int (V_{ds} - R_s i_{ds}) dt\end{aligned}\quad (4.1)$$

Where the direct and quadrature axis components of Voltage and current (in stator reference frame) are obtained from the 'abc' variables by using transformation as below

$$\begin{aligned}
 V_{qs} &= V_{as} \\
 V_{ds} &= \frac{1}{\sqrt{3}}(V_{cs} - V_{bs})
 \end{aligned}
 \tag{4.2}$$

$$\begin{aligned}
 i_{qs} &= i_{as} \\
 i_{ds} &= \frac{1}{\sqrt{3}}(i_{cs} - i_{bs})
 \end{aligned}
 \tag{4.3}$$

This transformation is applicable for voltage, current and flux linkage as well. To obtain uniformly rotating stator flux, note that the motor voltage have to be varied uniformly without steps too. This imposes a requirement of continuously variable stator voltage with infinite steps, which is not usually met by the inverter because it has only finite switching states.

4.3.3 Switching State of Inverter

Consider the inverter as shown in Fig. 4.2 below. The phase voltage V_{an} with respect to negative of the dc supply is determined by a set of switches, S_a , consisting of T_1 and T_4 as shown in Table 4.1. When the switching device T_1 and T_4 and their anti-parallel diodes are off, V_{an} is indeterminate. Such a situation is not encountered in practice and, hence, has not been considered.

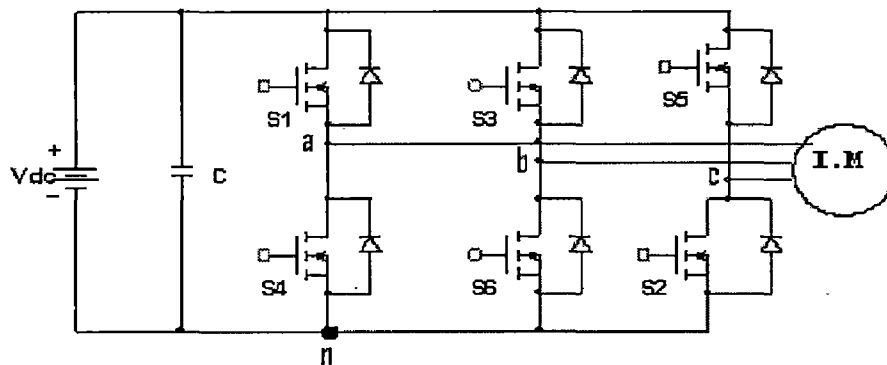


Fig.4.2: Three-phase Inverter

The switching of S_b and S_c sets for line b and c can be derived. The total number of switching states possible with S_a , S_b and S_c is eight; they are elaborated in Table 4.4 by using following relationships [14]:

Machine line voltages for a balanced system are

$$\begin{aligned} V_{ab} &= V_{an} - V_{bn} \\ V_{bc} &= V_{bn} - V_{cn} \\ V_{ca} &= V_{cn} - V_{an} \end{aligned} \quad (4.4)$$

Machine phases voltages for a balanced system are

$$\begin{aligned} V_{as} &= (V_{ab} - V_{ca})/3 \\ V_{bs} &= (V_{bc} - V_{ab})/3 \\ V_{cs} &= (V_{ca} - V_{bc})/3 \end{aligned} \quad (4.5)$$

and q and d axes voltage are given by

$$\begin{aligned} V_{qs} &= V_{as} \\ V_{ds} &= \frac{1}{\sqrt{3}}(V_{cs} - V_{bs}) \end{aligned} \quad (4.6)$$

T ₁	T ₄	S _a	V _{an}
on	Off	1	V _{dc}
off	On	0	0

Table 4.1: Switching states of inverter phase lag a

T ₃	T ₆	S _b	V _{bn}
on	Off	1	V _{dc}
off	On	0	0

Table 4.2: Switching states of inverter phase lag b

T ₅	T ₂	S _c	V _{cn}
on	Off	1	V _{dc}
off	On	0	0

Table 4.3: Switching states of inverter phase lag c

State	S_a	S_b	S_c	V_{an}	V_{bn}	V_{cn}	V_{ab}	V_{bc}	V_{ca}	V_{as}	V_{bs}	V_{cs}
I	1	0	0	V_{dc}	0	0	V_{dc}	0	$-V_{dc}$	$2/3V_{dc}$	$-1/3V_{dc}$	$-1/3V_{dc}$
II	1	0	1	V_{dc}	0	V_{dc}	V_{dc}	$-V_{dc}$	0	$1/3V_{dc}$	$1/3V_{dc}$	$1/3V_{dc}$
III	0	0	1	0	0	V_{dc}	0	$-V_{dc}$	V_{dc}	$-1/3V_{dc}$	$2/3V_{dc}$	$2/3V_{dc}$
IV	0	1	1	0	V_{dc}	V_{dc}	$-V_{dc}$	0	V_{dc}	$-2/3V_{dc}$	$1/3V_{dc}$	$1/3V_{dc}$
V	0	1	0	0	V_{dc}	0	$-V_{dc}$	V_{dc}	0	$-1/3V_{dc}$	$-1/3V_{dc}$	$-1/3V_{dc}$
VI	1	1	0	V_{dc}	V_{dc}	0	0	V_{dc}	$-V_{dc}$	$1/3V_{dc}$	$-2/3V_{dc}$	$-2/3V_{dc}$
VII	0	0	0	0	0	0	0	0	0	0	0	0
VIII	1	1	1	V_{dc}	V_{dc}	V_{dc}	0	0	0	0	0	0

Table 4.4: Inverter switching states and machine voltage

The stator q and d voltages for each state are shown in Fig. 4.3. The limited states of the inverter create distinct discrete movement of the stator-voltage phasor, V_s consisting of the resultant of V_{qs} and V_{ds} [14].

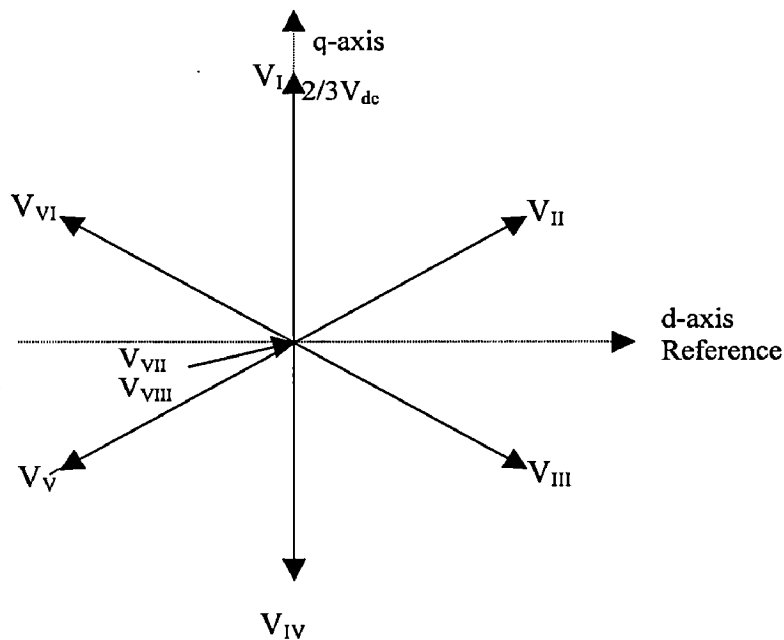


Fig. 4.3: The Inverter output voltage corresponding to switching states

An almost continuous and uniform flux phasor is feasible with these states, one due to their integration over time as seen from equation 4.1

For control of the voltage phasor both in its magnitude and phase, the requested voltage vector's phase and magnitude are sampled, say once every switching period. The

phase of requested voltage vector identifies the nearest two non-zero voltage vectors. The requested voltage vector can be synthesized by using fractions of the two nearest voltage vectors, which amounts to applying these two vectors, one at a time, for a fraction of the switching period. The nearest zero voltage vector to the two voltage vectors is applied for the remaining switching period. The duty cycle for each of the voltage vectors is determined by the phasor projection of the requested voltage vector onto the nearest zero voltage vectors. This method of controlling the input voltages to the machine through a synthesis of voltage phasor rather than the individual line-to-line voltages has the advantages of: i) not using pulse width modulation carrier-frequency signal, ii) higher fundamental voltages compared to sine-triangle PWM, based controllers, iii) given the switching frequency, the switching frequency losses are minimized, and iv) lower voltage and current ripples. This method of switching the inverter is known as space vector modulation [19][20].

4.3.4 Flux Control

A uniform rotating stator flux is desirable, and it occupies one of the sextants (in the phasor diagram shown in Fig 4.4) at any time.

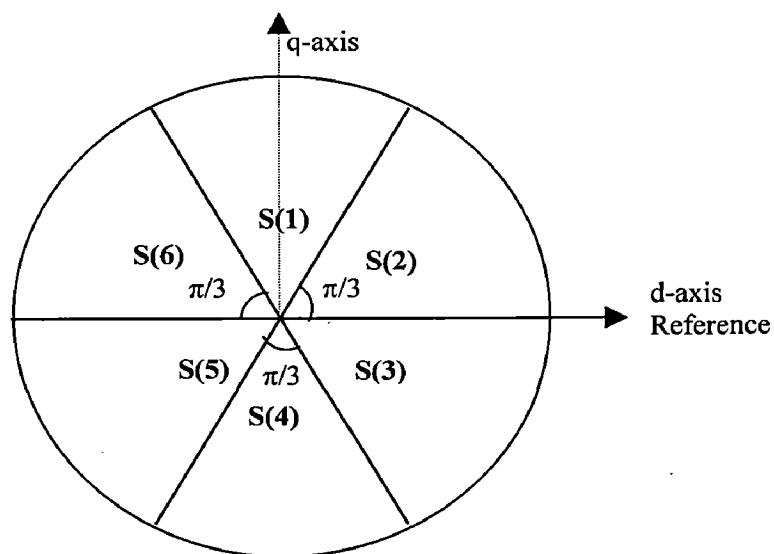


Fig 4.4: Division of sector for stator flux linkage identification

The stator flux phasor has a magnitude of λ_s , with an instantaneous position of θ_{fs} . The corresponding d and q axes component are λ_{ds} and λ_{qs} respectively. Assuming that

a feedback of stator flux is available, its place is identified from its position. Then the influencing voltage phasor is identified by giving a 90° phase shift. For example, if the stator-flux phasor is in sextant '2', the right influencing voltage phasor has to be either VI or I. voltage phasor I is $90^\circ - \theta_{fs}$ and VI is $150^\circ - \theta_{fs}$ from the flux phasor. One of these two sets increase λ_s , the other decreases λ_s . This is found from following explanation obtained from Fig. 4.5[17]

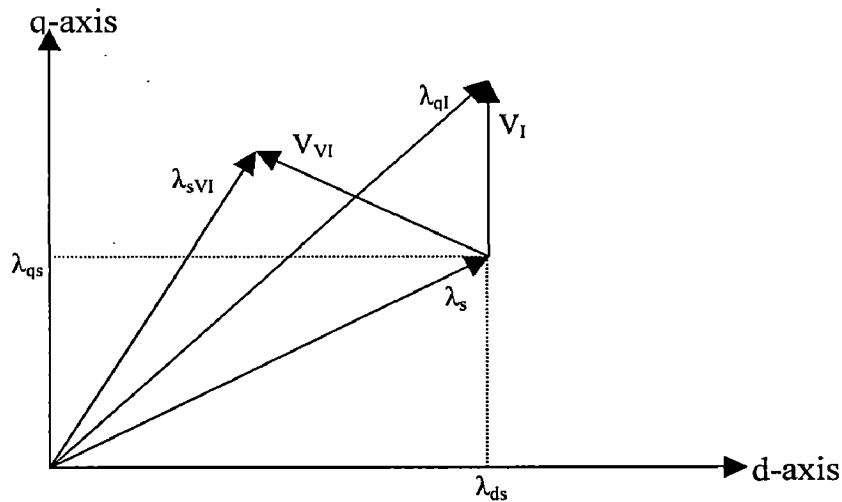


Fig. 4.5: Effect of switching V_I and V_{VI} on stator-flux phasor

Consider the effect of switching voltage phasor set I, V_I , the phasor set VI, V_{VI} . As seen from the phasor diagram, in the case of set I, the flux phasor increase in magnitude from λ_s to λ_{sI} ; in the case of set VI, it decreases to λ_{sVI} . This implies that the closer voltage phasor set increases the flux and farther voltage-phasor set decreases the flux, but not that both of them advance the flux phasor in position. Similarly for all other sextants, the switching is developed. A flux error is processed through a window comparator to produce digital o/p (let it be S_λ) according to following condition and determines which voltage phasor has to be called[17].

Condition	S_λ
$(\lambda_s^* - \lambda_s) > H\lambda_s$	1
$(\lambda_s^* - \lambda_s) \leq H\lambda_s$	0

Table 4.5: Stator Flux Hysteresis Window output

4.3.5 Torque Control

Over and above the flux control, the control of electromagnetic torque is required for high-performance drive. It is achieved as follows.

Torque control is exercised by comparison of the command torque to the torque measured from the stator flux linkages and stator currents as

$$T_e = \frac{3}{2} \frac{P}{2} (\lambda_{ds} i_{qs} - \lambda_{qs} i_{ds}) \quad (4.7)$$

The torque error is processed through a window comparator to produce digital o/p (let it be S_T) according to following condition.

Condition	S_T
$(T_e^* - T_e) > HT_e$	1
$-HT_e < (T_e^* - T_e) < HT_e$	0
$(T_e^* - T_e) < -HT_e$	-1

Table 4.6: Torque Hysteresis Window output

Where HT_e is acceptable error in torque. When the torque error is exceeds HT_e , It is time to increase the torque, denoting it with a +1 signal. If the torque error is between positive and negative torque window, then the voltage phasor could be at zero state. If the torque error is bellow $-H\lambda_s$, it amounts to calling for regeneration, signified by -1 logic signal[13][14].

Combining the flux error output S_λ , the torque error output S_T , and the sextant of the flux phasor $S(k)$, a switching table can be realized to obtain the switching states of the inverter; it is given in Table 4.7. The algorithm for $S(k)$ is shown in Table 4.8 where the field angle can be calculated as

$$\theta_{fs} = \tan^{-1} \left(\frac{\lambda_{qs}}{\lambda_{ds}} \right) \quad (4.8)$$

S_λ	S_T	S (1)	S (2)	S (3)	S (4)	S (5)	S (6)
1	1	VI (1,1,0)	I (1,0,0)	II (1,0,1)	III (0,0,1)	IV (0,1,1)	V (0,1,0)
1	0	VIII (1,1,1)	VII (0,0,0)	VIII (1,1,1)	VII (0,0,0)	VIII (1,1,1)	VII (0,0,0)
1	-1	II (1,0,1)	III (0,0,1)	IV (0,1,1)	V (0,1,0)	VI (1,1,0)	I (1,0,0)
0	1	V (0,1,0)	VI (1,1,0)	I (1,0,0)	II (1,0,1)	III (0,0,1)	IV (0,1,1)
0	0	VII (0,0,0)	VIII (1,1,1)	VII (0,0,0)	VIII (1,1,1)	VII (0,0,0)	VIII (1,1,1)
0	-1	III (0,0,1)	IV (0,1,1)	V (0,1,0)	VI (1,1,0)	I (1,0,0)	II (1,0,1)

Table 4.7 : Switching states for possible S_λ , S_T and $S(k)$

θ_{fs} (field angle)	$S(k)$ (sextant)
$0 < \theta_{fs} \leq \pi/3$	S(2)
$-\pi/3 < \theta_{fs} \leq 0$	S(3)
$-2\pi/3 < \theta_{fs} \leq -\pi/3$	S(4)
$-\pi < \theta_{fs} \leq -2\pi/3$	S(5)
$2\pi/3 < \theta_{fs} \leq \pi$	S(6)
$\pi/3 < \theta_{fs} \leq 2\pi/3$	S(1)

Table 4.8: Flux Phasor Sextants

Consider the first column corresponding to $S(k) = S(1)$. The switching states of the inverter are indicated in parentheses; they correspond to S_a , S_b , and S_c . the flux error signal indicates 1, which means the flux is less than its requested value and therefore the flux phasor has to be increased. At the same time, torque error is positive, asking for an increase. Merging these two with the position of the flux phasor in S(1), the phase voltage I and VI satisfy the requirements only if the flux is within the first 30° of sextant S(1). In the second 30° , note that the voltage phasor I will increase the flux-phasor magnitude but will retard it in phase. This will result in a reduction of the stator frequency and reversal of the direction of torque. The control requires the advancement of the flux-phasor in the same direction (i.e. counterclockwise in this discussion); that

could be satisfied only by voltage phasor VI in this 30° . Voltage phasor VI is the one satisfying the uniform requirements throughout the sextant S(1), so the voltage phasor VI is chosen for S_T and S_λ to be equal to +1 with the flux phasor in sextant S(1). When the torque error is zero, the only logical choice is to apply zero line voltage; because the previous state had two +1 states, it is easy to achieve zero line voltage by choosing the switching state VIII with all one. If the torque error becomes negative with $S_T = -1$, the machine has to regenerate, with a simultaneous increase in flux phasor due to $S_\lambda = 1$; hence the voltage phasor is retarded close to the flux phasor, and, hence, switching state II(1,0,1) is selected.

If $S_\lambda = 0$ (i.e., the flux phasor has exceeded its request by the hysteresis band amount), then it has to be decreased to match its requested value by choosing a voltage phasor away from flux phasor, i.e., V. this accelerates the flux phasor and increases the slip speed, resulting also in an increase of electromagnetic torque, thus satisfying $S_T = 1$ demand. When $S_T = 0$, reach zero line-voltage states by going to VII, because V contained two zero states in it. If $S_T = -1$, then regenerate, increasing the negative torque but decreasing the flux phasor; this is achieved by retarding the voltage phasor behind the flux phasor, but far away from it, and hence III is chosen. Note that it has two zeros in it, and, therefore, transition from VII to III requires a change of only one switch signal[17].

CHAPTER 5

SIMULATION RESULTS AND DISCUSSION

Induction motor drive, proposed in Figure 4.1, is simulated using the software package Matlab/Simulink programming environment, in which machine is modelled with given machine parameter. The physical parameter variations are neglected. The speed PI controller and hysteresis band for torque and flux control has been included in simulation. Every instant of a inverter power device switching on and off is decided with the these hysteresis band . Fig. 5.1 shows the block diagram of simulated drive in MATLAB.

The performance of Direct Torque Control induction motor fed by voltage source inverter is investigated under different load condition (i.e. constant load and traction type load). The closed loop operation is performed to control the speed and torque of induction motor. The simulation result of drive is obtained in constant torque region and constant power region under different load condition and different speed reference.

5.1 SIMULATION RESULT IN CONSTANT TORQUE REGION

Fig 5.2 to Fig. 5.16 shows the simulation results of transient and steady state response of motor in constant torque region.

5.1.1 Step change in load

Fig 5.2 to Fig 5.6 show the simulation results when the load is steeply changed from no-load to 0.7 p.u. load. It show transient and steady state response of the induction motor characteristics like torque in Fig 5.2, speed in Fig 5.3, stator phase current Fig 5.4, stator flux in Fig 5.5 and stator flux sector in Fig 5.6. The motor is initially at rest and given a speed command of 0.8 p.u. at no load. The motor take around 0.39 sec to obtain speed reference while in the same time the electromagnetic torque remains constant as maximum torque (T_m). As soon as the speed becomes steady state (Fig 5.3), the electromagnetic torque becomes equal to load torque (Fig 5.2). Under the same speed, the load torque increase from no load to 0.7 p.u load at $t=0.69$ sec. then electromagnetic torque become equal to 0.8 p.u. while the speed slightly decreased. Under this variation

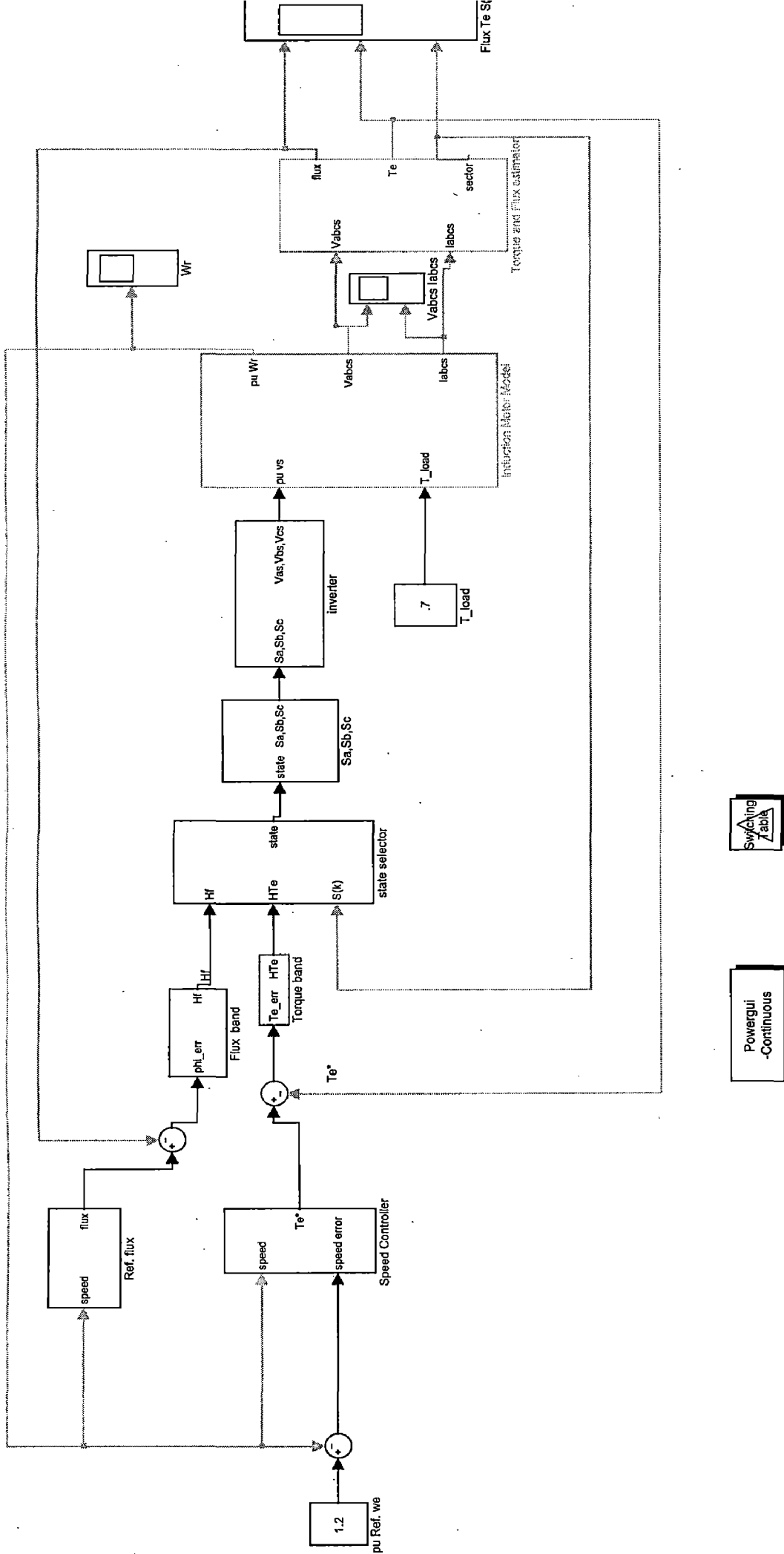


Fig 5.1 Simulation Bloch Diagram for Direct Torque Control

of load torque, the stator current (Fig 5.4) varied according to electromagnetic torque while the stator flux (Fig 5.5) remain constant irrespective of electromagnetic torque.

5.1.2 Step change in speed

Fig 5.7 to Fig 5.11 show the simulation results when the speed reference is steeply changed from 0.5 p.u. to 0.9 p.u. It show transient and steady state response of the induction motor characteristics like torque in Fig 5.7, speed in Fig 5.8, stator phase current Fig 5.9, stator flux in Fig 5.10 and stator flux sector in Fig 5.11. As the reference speed taken as 0.5 p.u. at no load, the characteristics is similar as in previous case until steady state response. Under the same load torque, the speed reference increase from 0.5 p.u. to 0.9 p.u at $t=0.454$ sec. then electromagnetic torque reached at its maximum value instantaneously and maintain it until rotor speed become reference speed. As soon as the speed becomes steady state (Fig 5.8), the electromagnetic torque becomes equal to load torque (Fig 5.7). Under this variation of speed reference, the stator current (Fig 5.9) varied according to electromagnetic torque while the stator flux (Fig 5.5) remain constant irrespective of reference speed variation (Fig 5.10).

5.1.3 Traction type load

In traction system, the load is varied and depends upon speed of motor. Fig 5.12 to Fig 5.16 show the simulation results when load is varied as

$$T_l = (0.6 * \omega_r * \omega_r + 0.1). \quad (5.1)$$

It show transient and steady state response of the induction motor characteristics like torque in Fig 5.12, speed in Fig 5.13, stator phase current Fig 5.14, stator flux in Fig 5.15 and stator flux sector in Fig 5.16. . The motor is initially at rest and given a speed command of 0.6 p.u. The motor take around 0.32 sec to obtain speed reference while in the same time the electromagnetic torque remains constant as maximum torque (T_m) irrespective of load variation. As soon as the speed becomes steady state (Fig 5.13), the electromagnetic torque becomes equal to load torque according to equation (5.1). Again it is observed that although the load is varied continuously but electromagnetic torque obtained its maximum value until rotor speed become equal to reference speed and then

load torque with in a small time. Under this variation of load torque, the stator current (Fig 5.14) varied according to electromagnetic torque while the stator flux (Fig 5.15) remain constant irrespective of load torque.

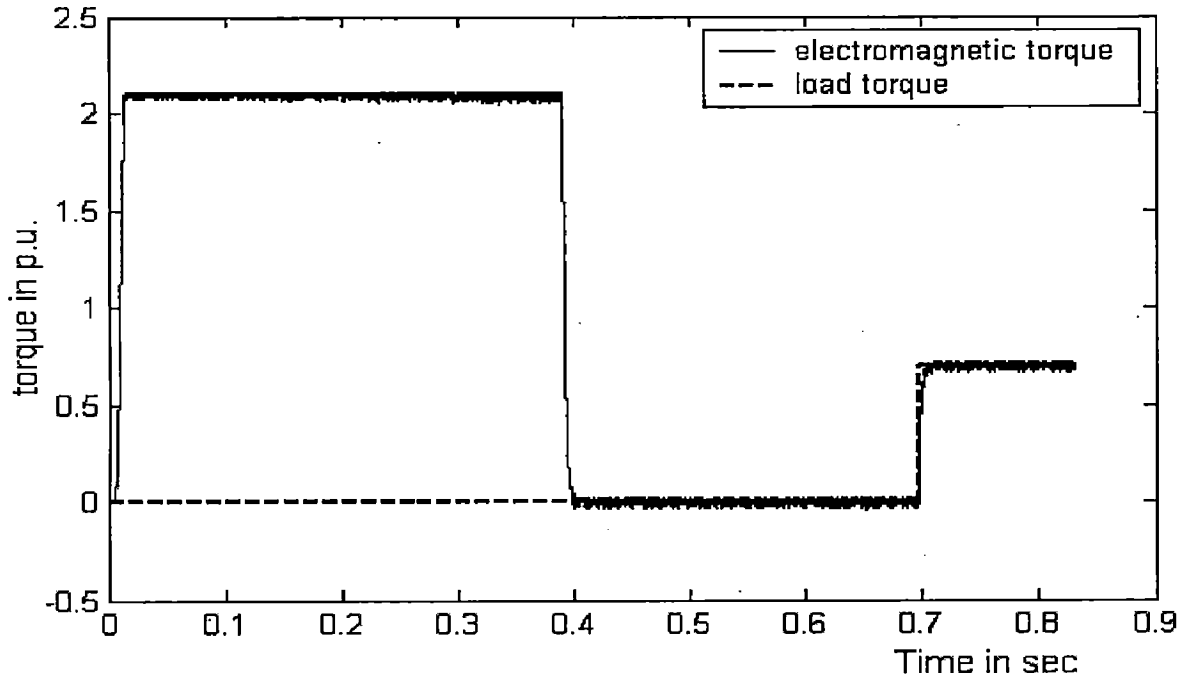


Fig. 5.2 Torque response when step change in load below base speed.

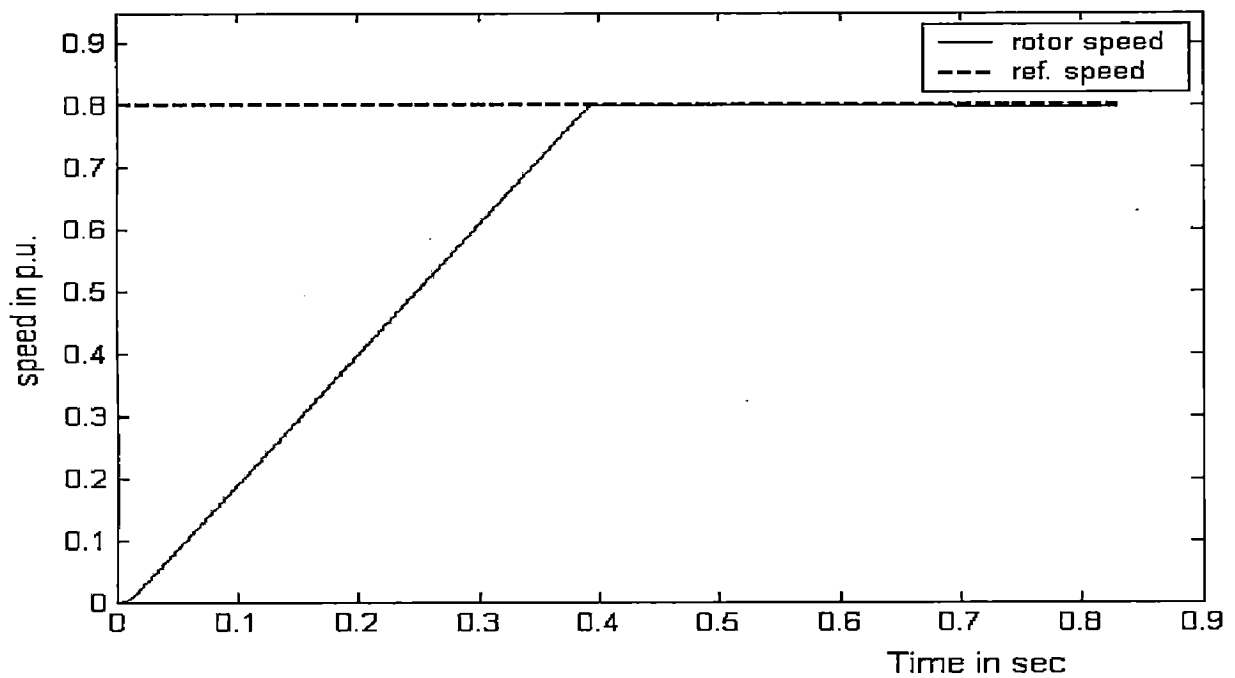


Fig. 5.3 Rotor speed response when step change in load below base speed.

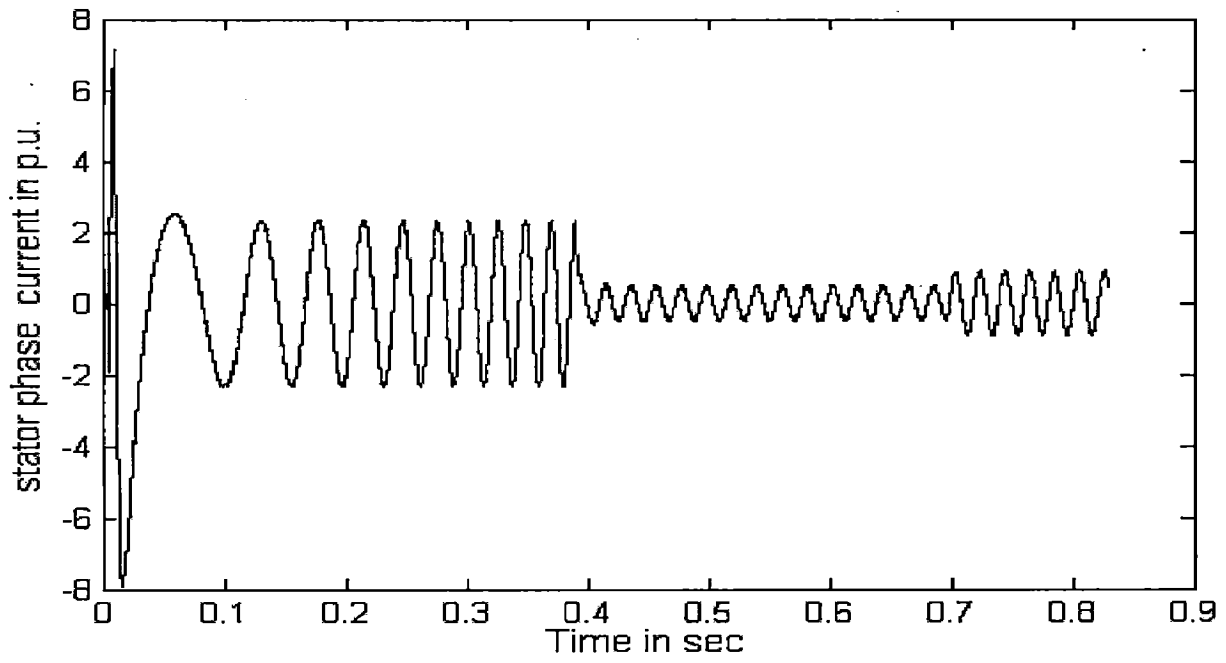


Fig. 5.4 Stator phase current (I_{as}) response when step change in load below base speed.

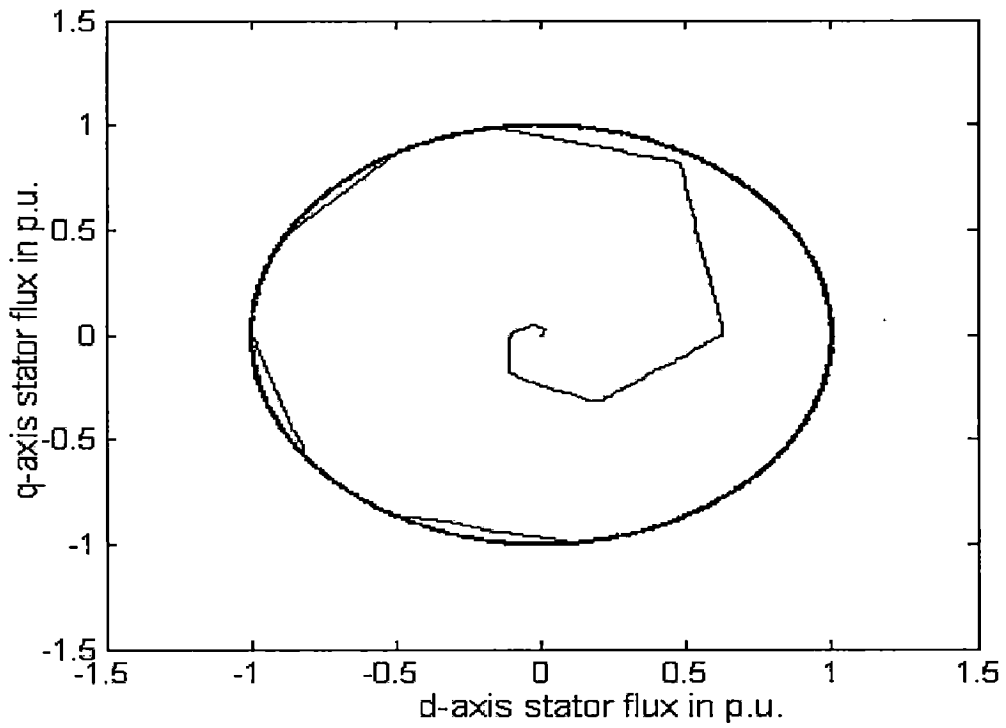


Fig. 5.5(a): d-q Stator flux loci

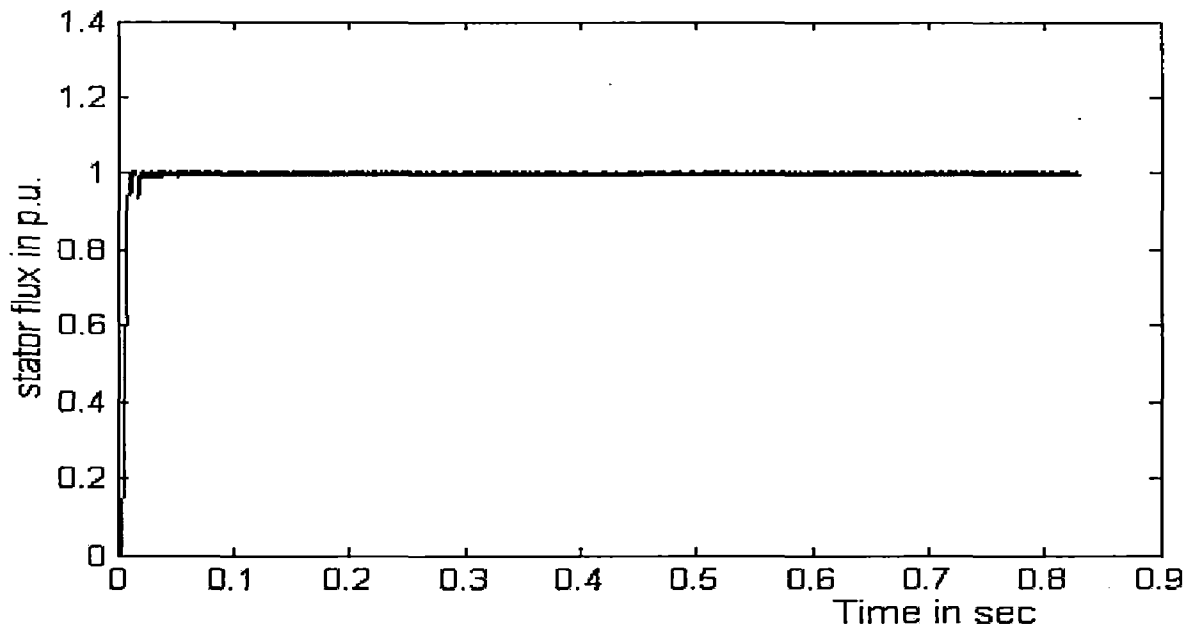


Fig. 5.5(b): Stator flux magnitude

Fig. 5.5 Stator flux response when step change in load below base speed.

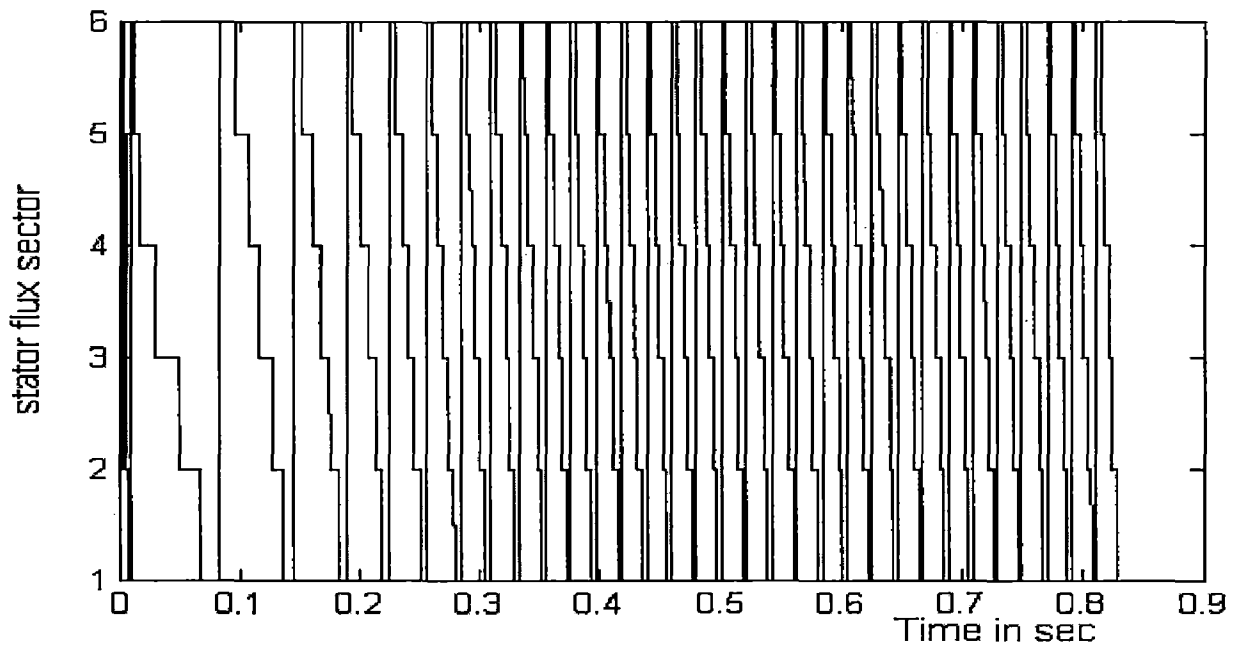
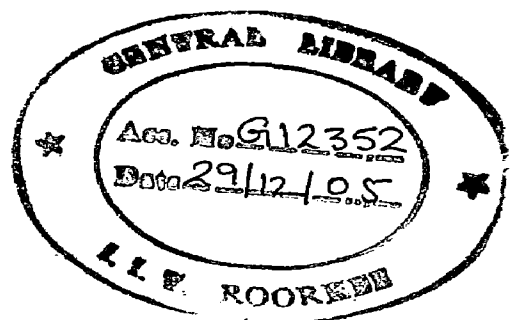


Fig. 5.6 Stator flux sector response when step change in load below base speed.



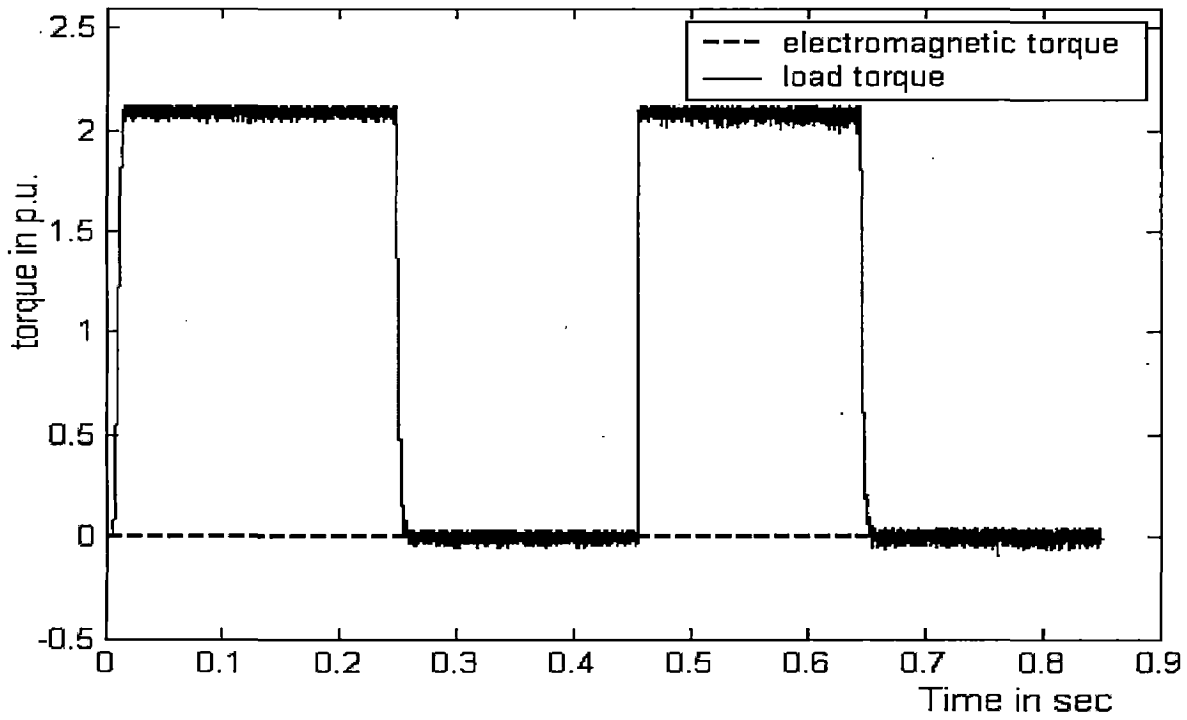


Fig. 5.7: Torque response when step change in speed below base speed.

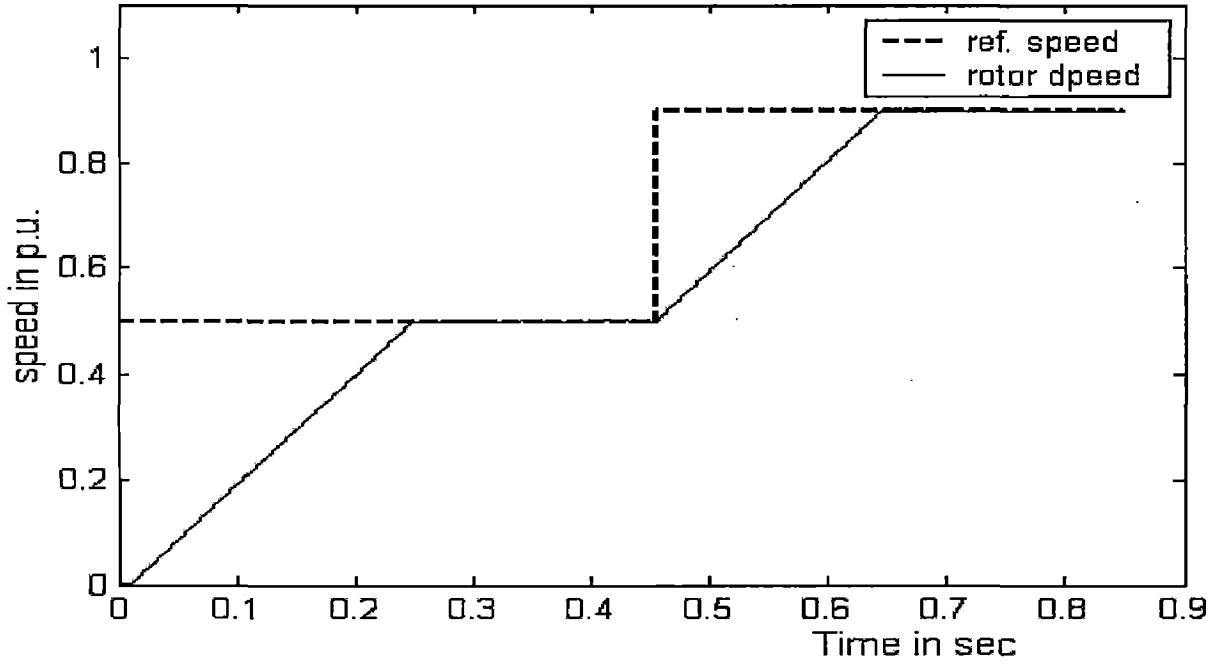


Fig. 5.8: Rotor speed response when step change in speed below base speed.

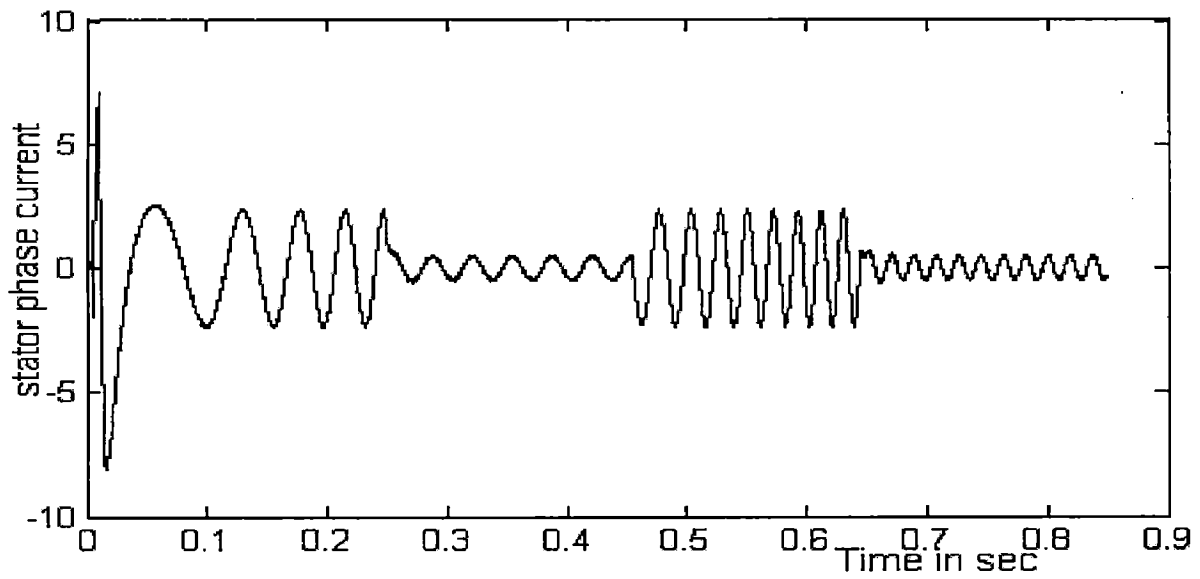


Fig. 5.9: Stator phase current (I_{as}) response when step change in speed below base speed.

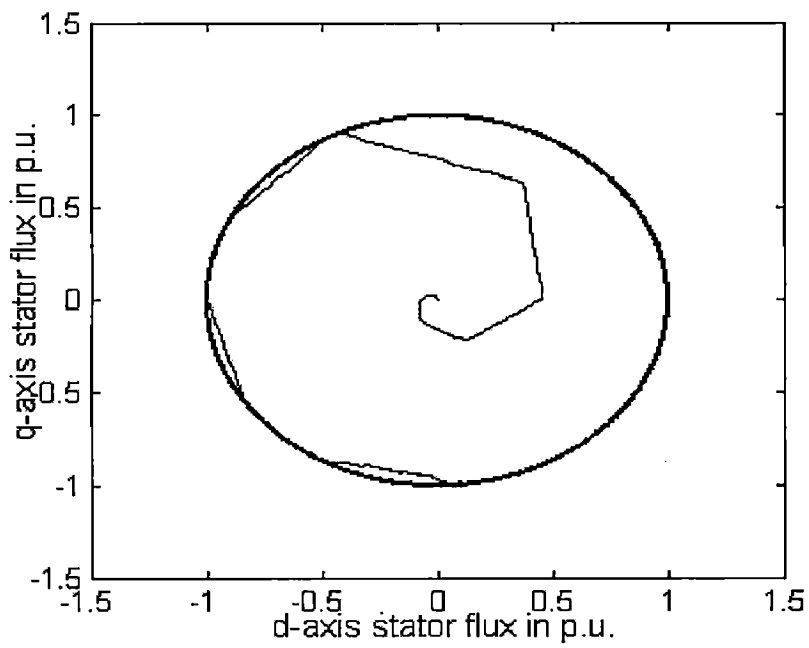


Fig. 5.10(a) : d-q Stator flux loci

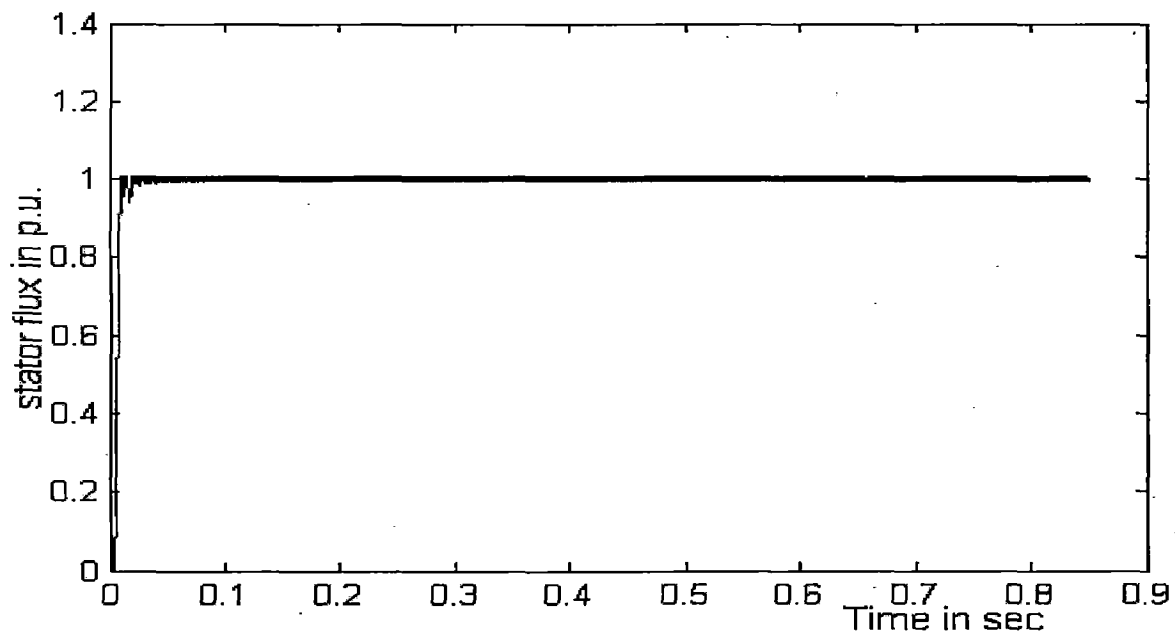


Fig. 5.10(b): Stator flux magnitude

Fig. 5.10: Stator flux response when step change in speed below base speed.

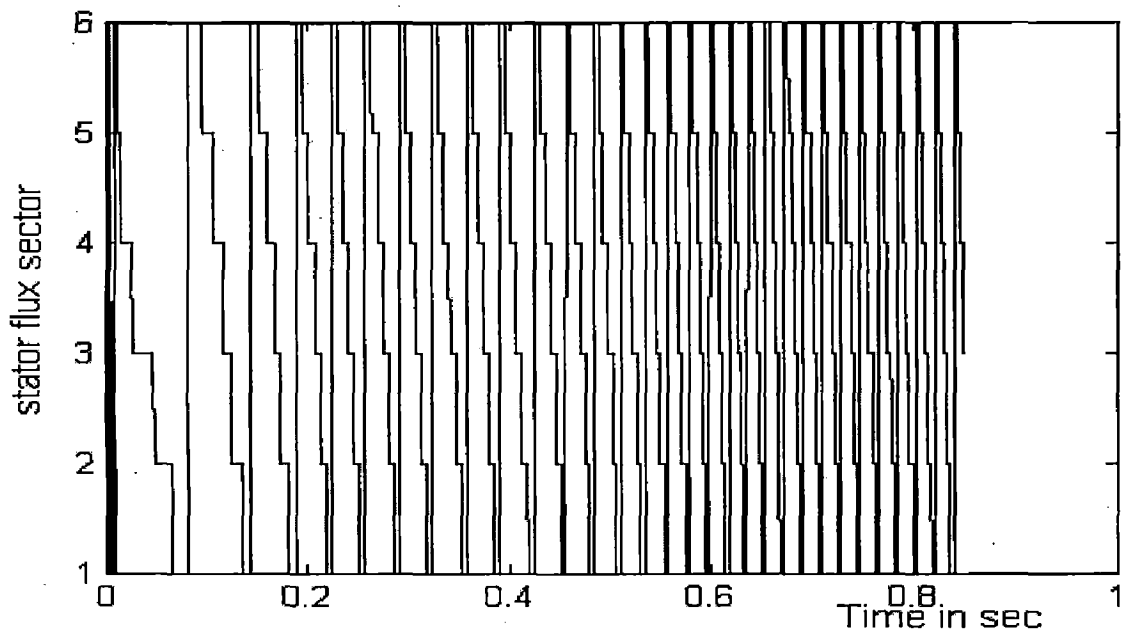


Fig. 5.11: Stator flux sector response when step change in speed below base speed.

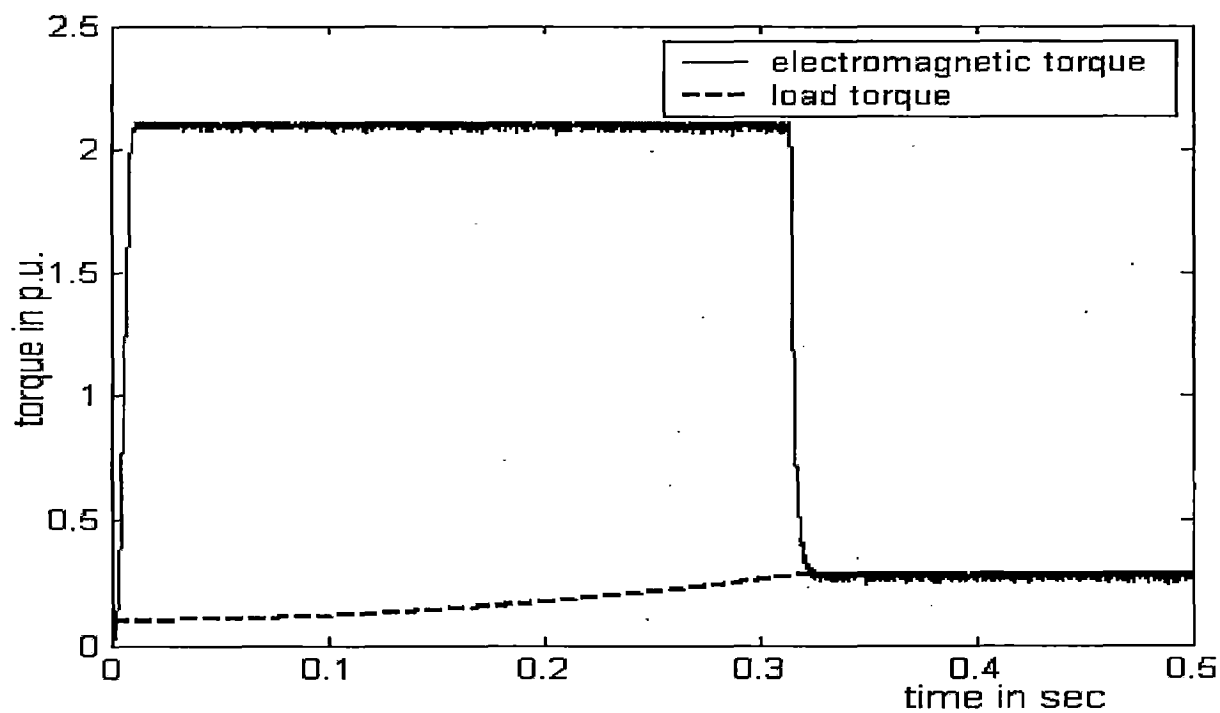


Fig. 5.12: Torque response under traction type load below base speed.

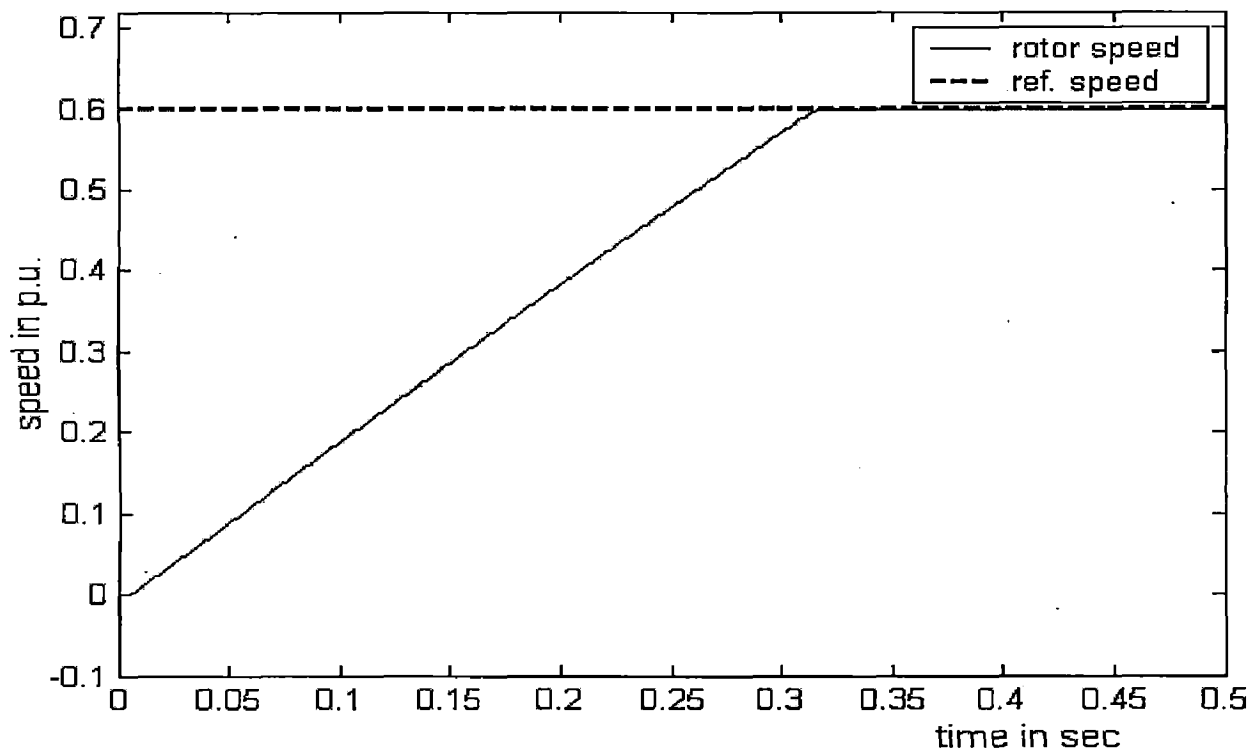


Fig. 5.13: Rotor speed response under traction type load below base speed.

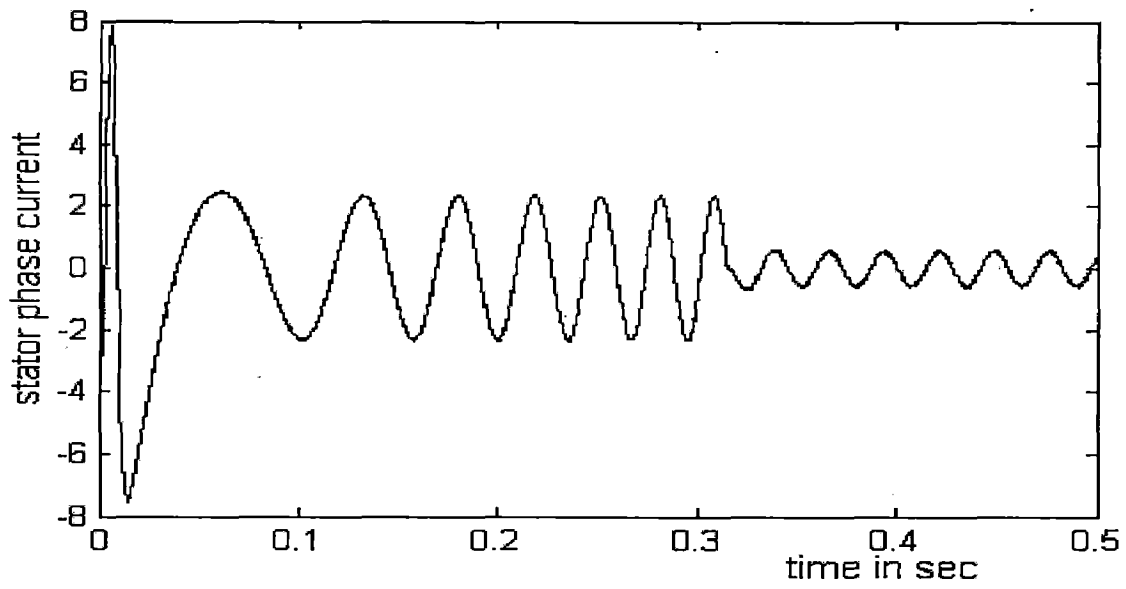


Fig. 5.14: Stator phase current (I_{as}) response under traction type load below base speed

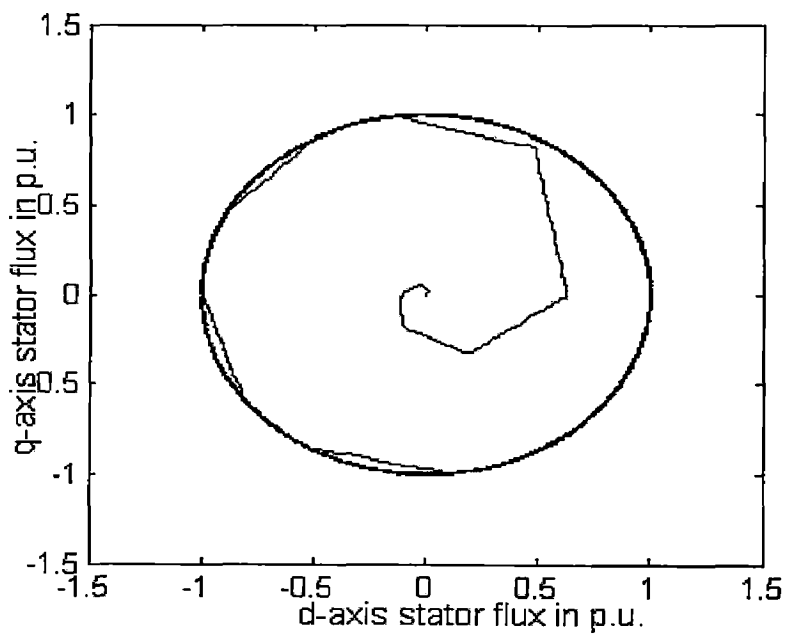


Fig. 5.15(a) : d-q Stator flux loci

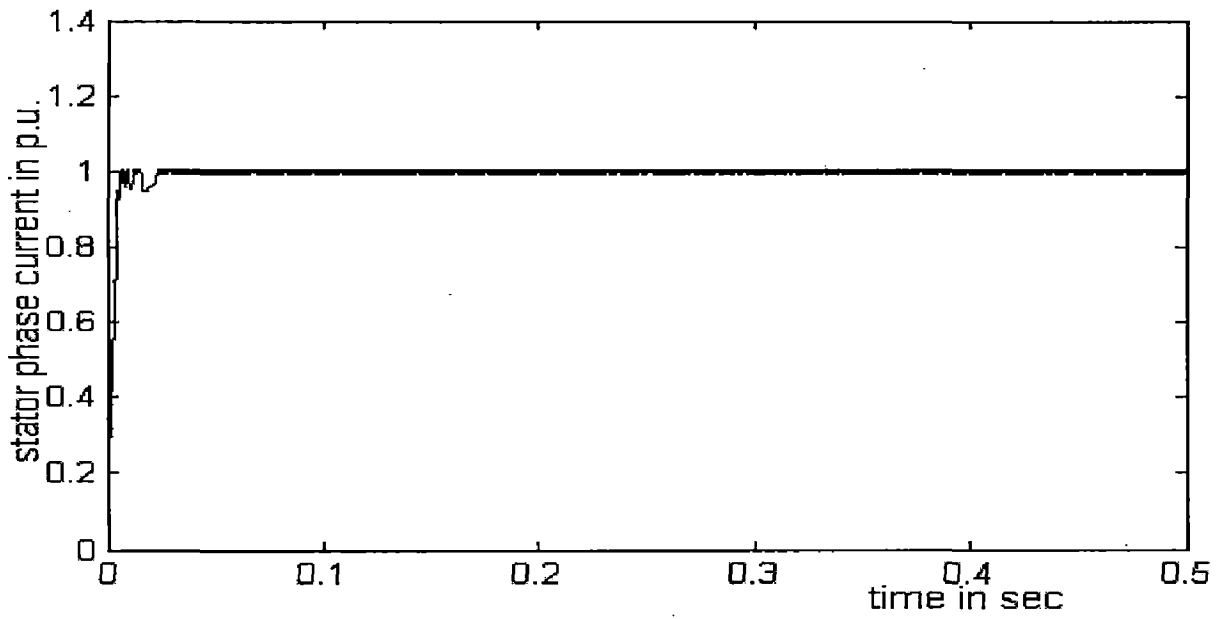


Fig. 5.15(b): Stator flux magnitude

Fig. 5.15: Stator flux response under traction type load below base speed.

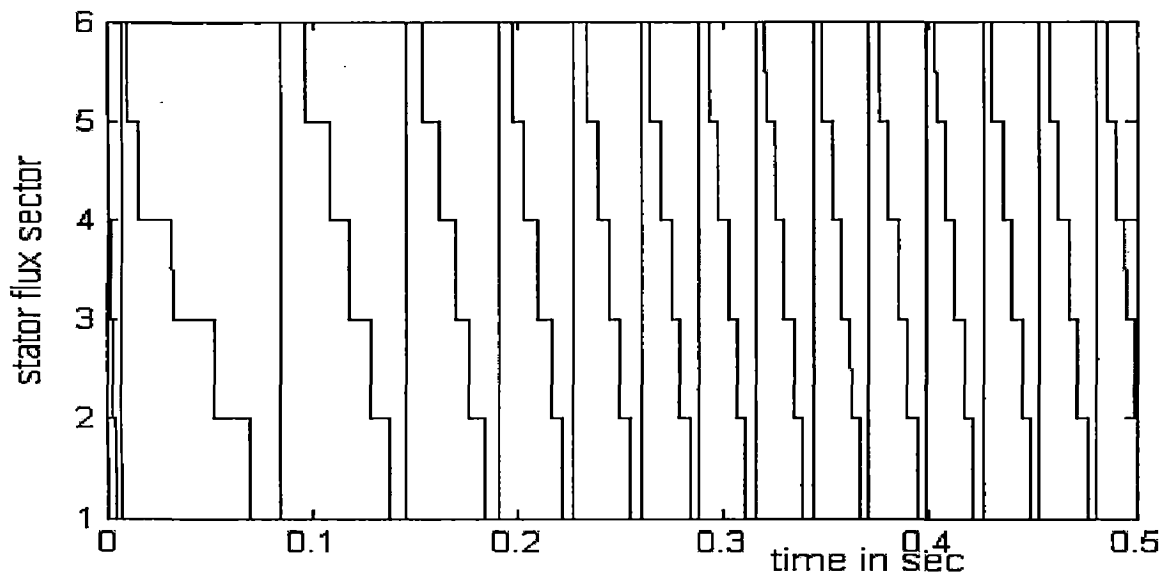


Fig. 5.16: Stator flux sector response under traction type load below base speed.

5.2 SIMULATION RESULT IN FLUX WEAKENING REGION

Fig 5.17 to Fig. 5.31 shows the simulation results of drive performance under flux weakening region. The result is taken in different conditions of speed and load torque.

5.2.2 Step change in load

Fig 5.17 to Fig 5.21 show the simulation results when the load is steeply changed from no-load to 0.8 p.u. load while motor is running above base speed. In this case, reference speed is 1.3 p.u., which is more than base speed. Here it is observed that upto base speed the electromagnetic torque and stator flux remain constant to its maximum value. After the base speed the electromagnetic torque and stator flux decrease in such a manner that power remain constant. As soon as motor reaches to reference speed, the torque become equal to no load and flux become constant depend upon speed. Here it is observed that the stator current remain constant until the speed become reference speed and this the current reduced to load current. Under the same speed, the load torque increase from no load to 0.8 p.u load at $t=0.95\text{sec}$. then electromagnetic torque become equal to 0.8 p.u. while the speed slightly decreased.

5.2.2 Step change in speed

Fig 5.22 to Fig 5.26 show the simulation results when the reference speed is steeply changed from 1.2 p.u. to 1.6 p.u. while motor is running above base speed. Here it is observed that As the reference speed taken as 1.2 p.u. at no load, the characteristics is similar as in previous case until steady state response. Under the same load torque, the speed reference increase from 1.2 p.u. to 1.6 p.u at $t=0.8\text{sec}$. then electromagnetic torque reached at its maximum value instantaneously corresponding to rotor speed and varied with rotor speed as shown in fig. 5.22. Here it is also observed that stator current obtain its maximum value whenever motor is running in transient condition.

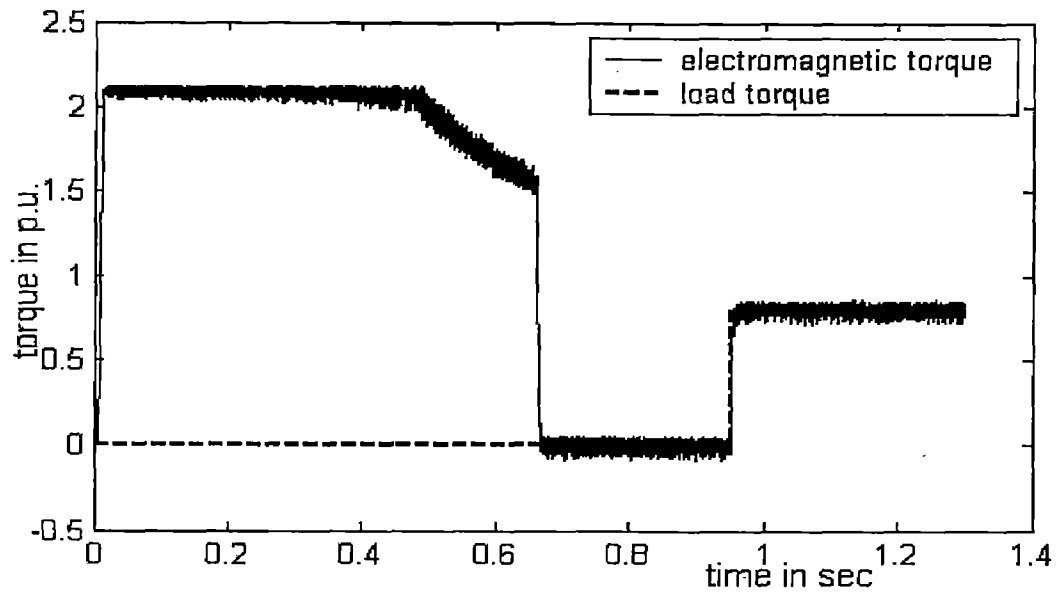


Fig. 5.17: Torque response when step change in load above base speed.

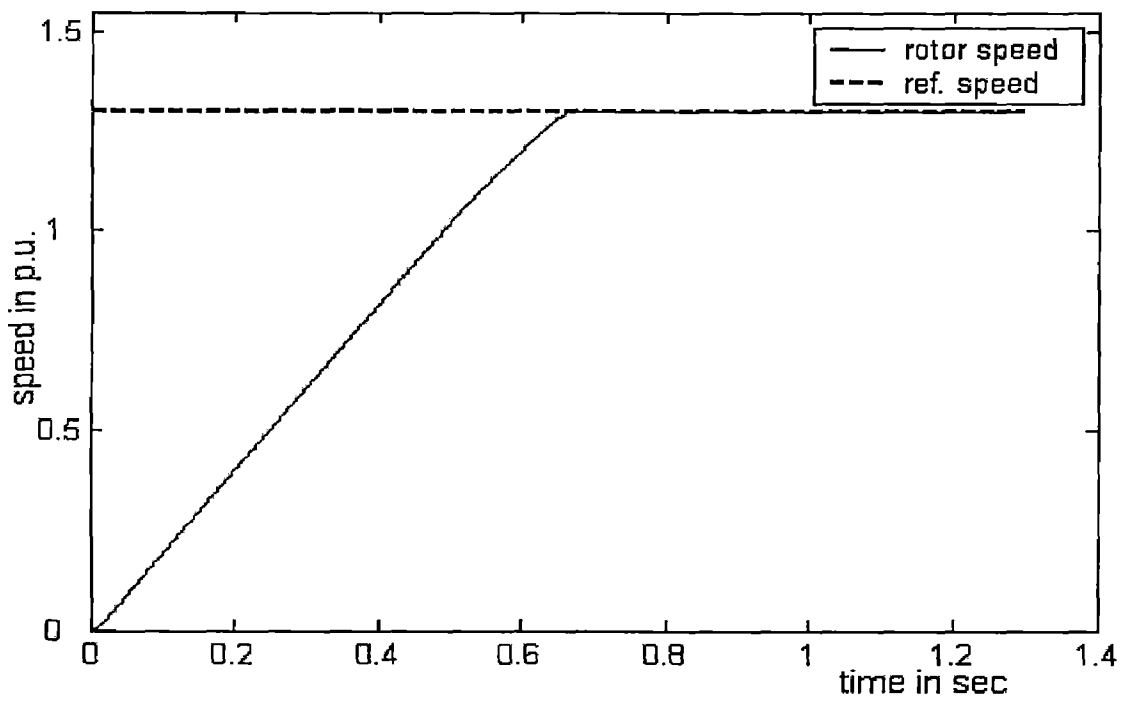


Fig. 5.18: Rotor speed response when step change in load above base speed.

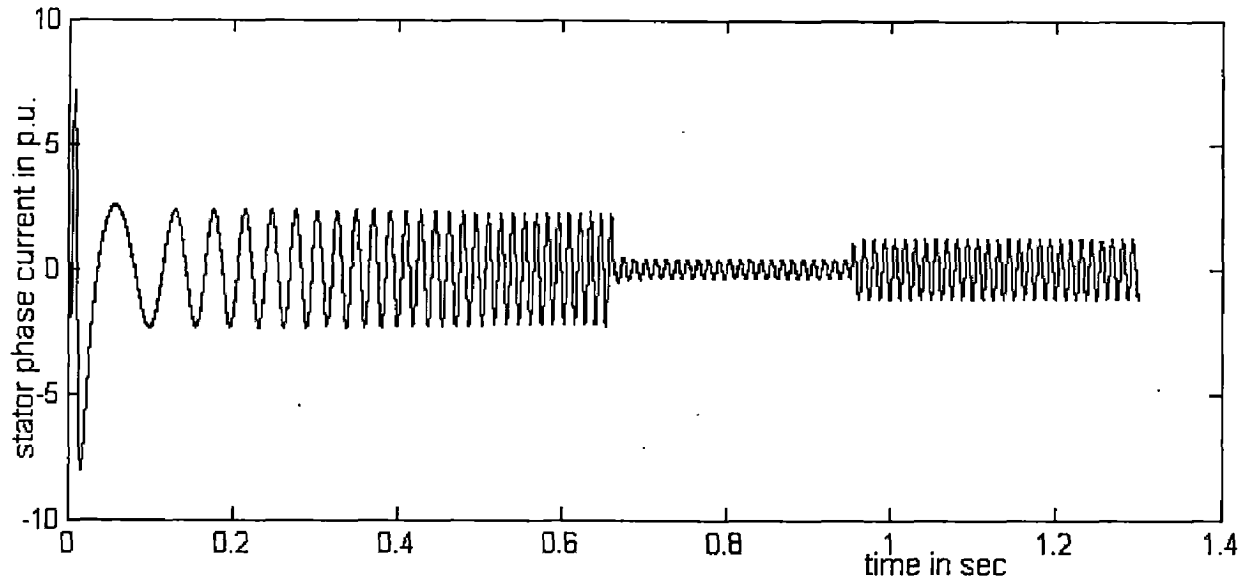


Fig. 5.19: Stator phase current (I_{as}) response when step change in load above base speed.

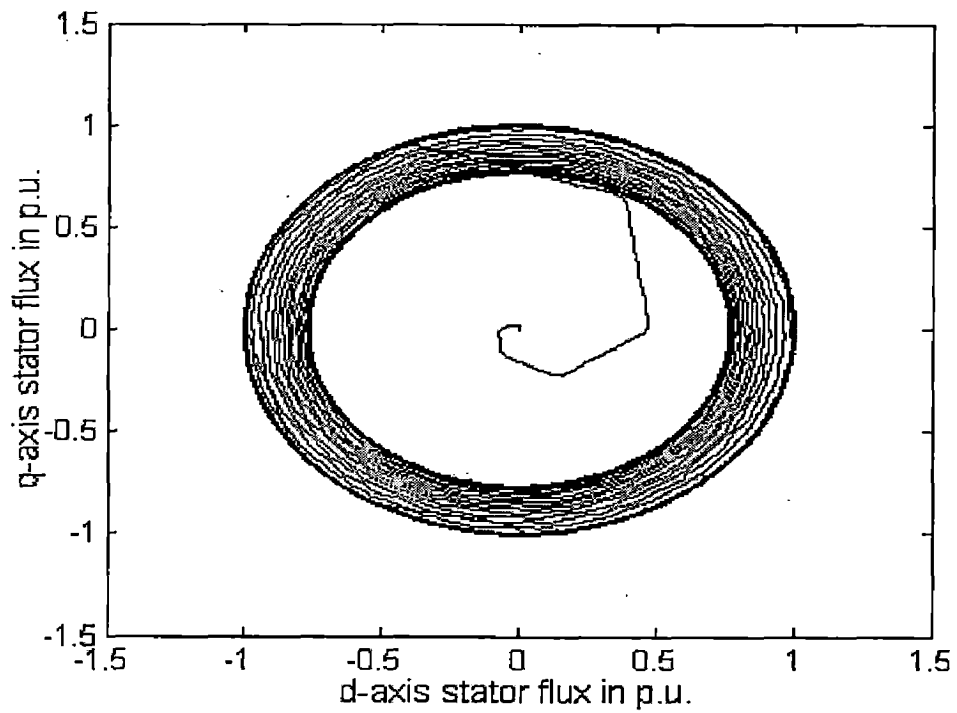


Fig. 5.20(a) : d-q Stator flux loci

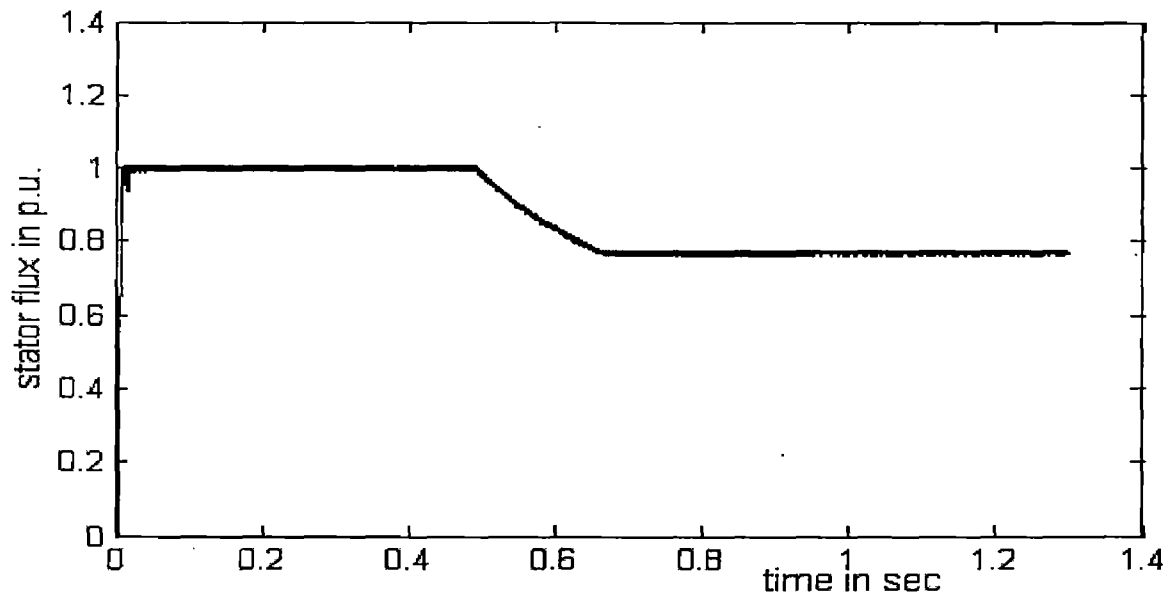


Fig. 5.20(b): Stator flux magnitude

Fig. 5.20: Stator flux response when step change in load above base speed.

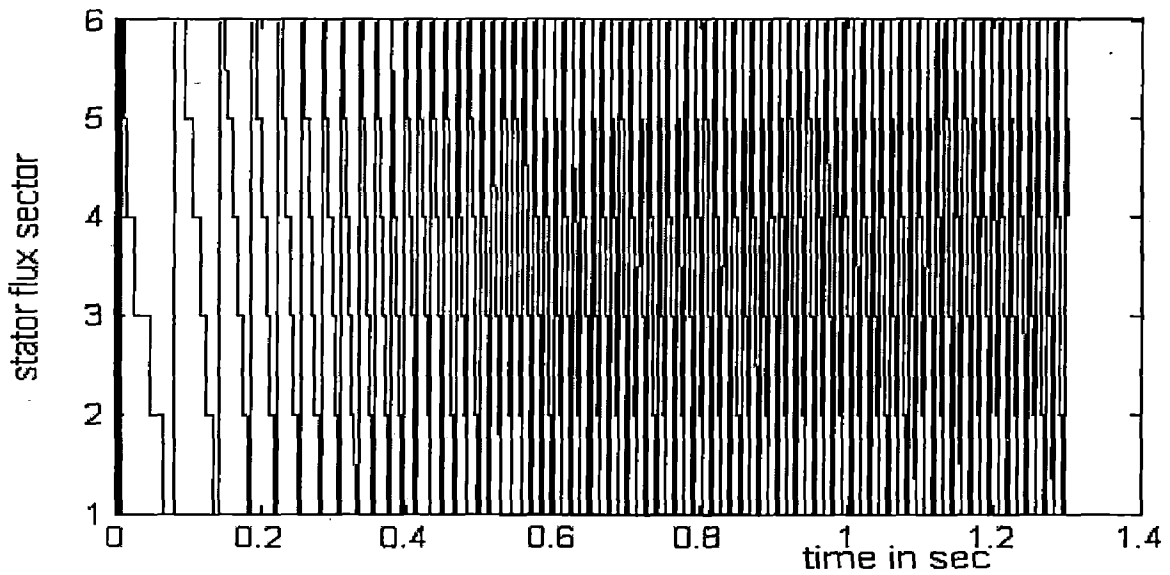


Fig. 5.21: Stator flux sector response when step change in load above base speed.

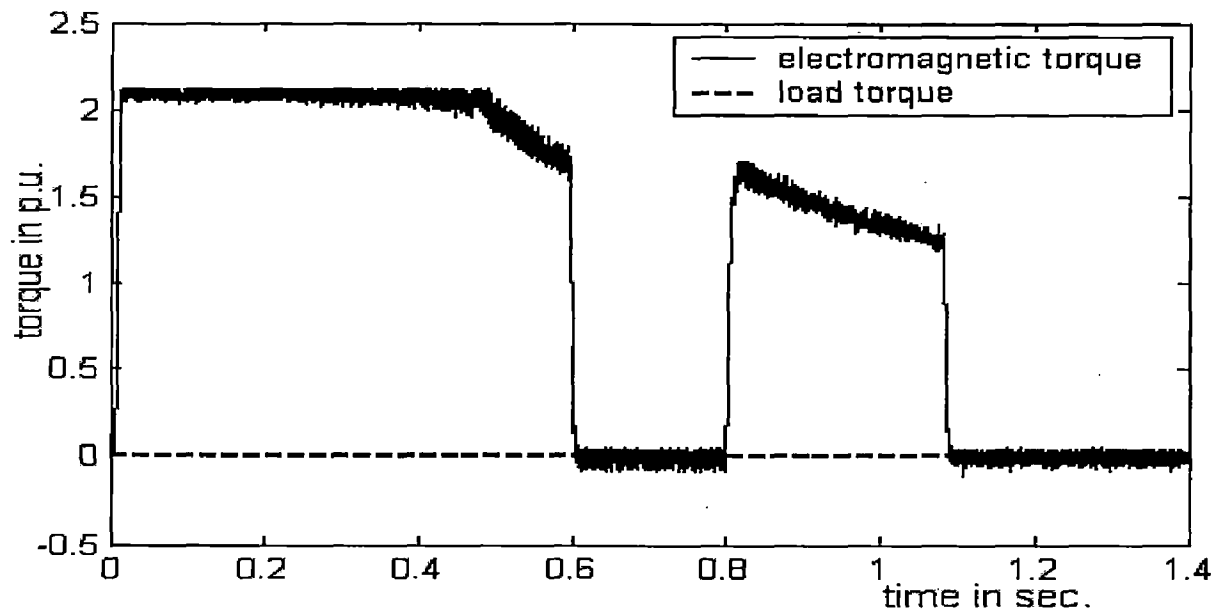


Fig. 5.22: Torque response when step change in speed above base speed.

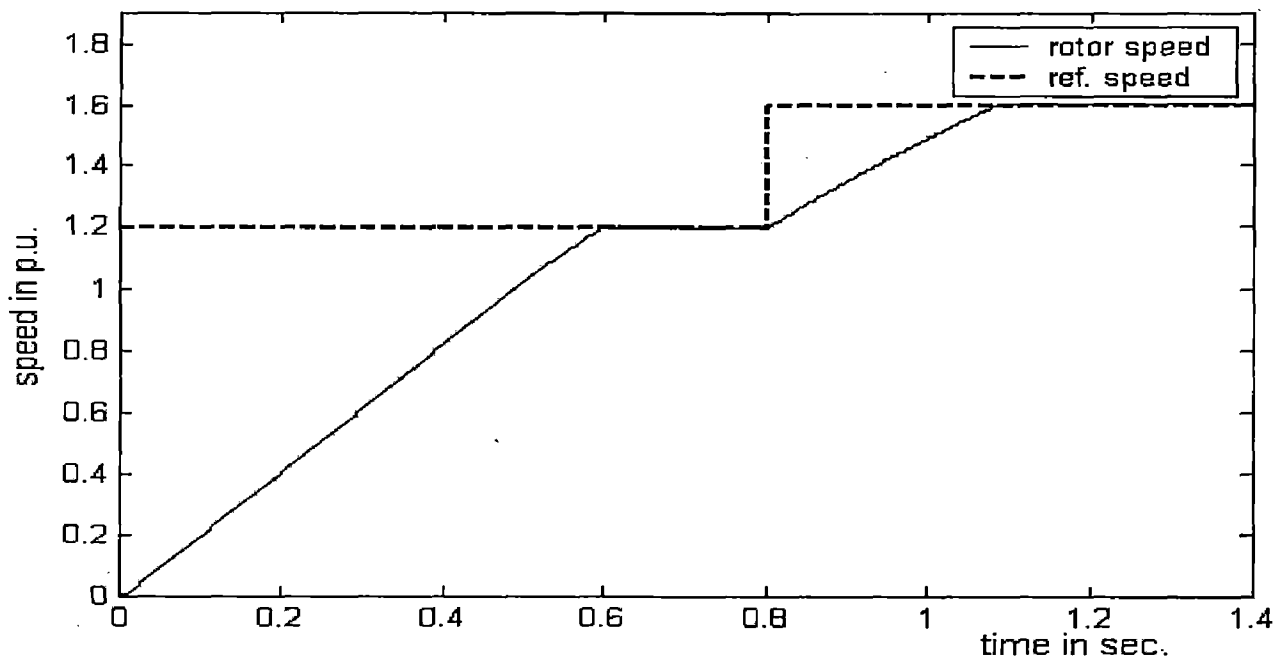


Fig. 5.23: Rotor speed response when step change in speed above base speed.

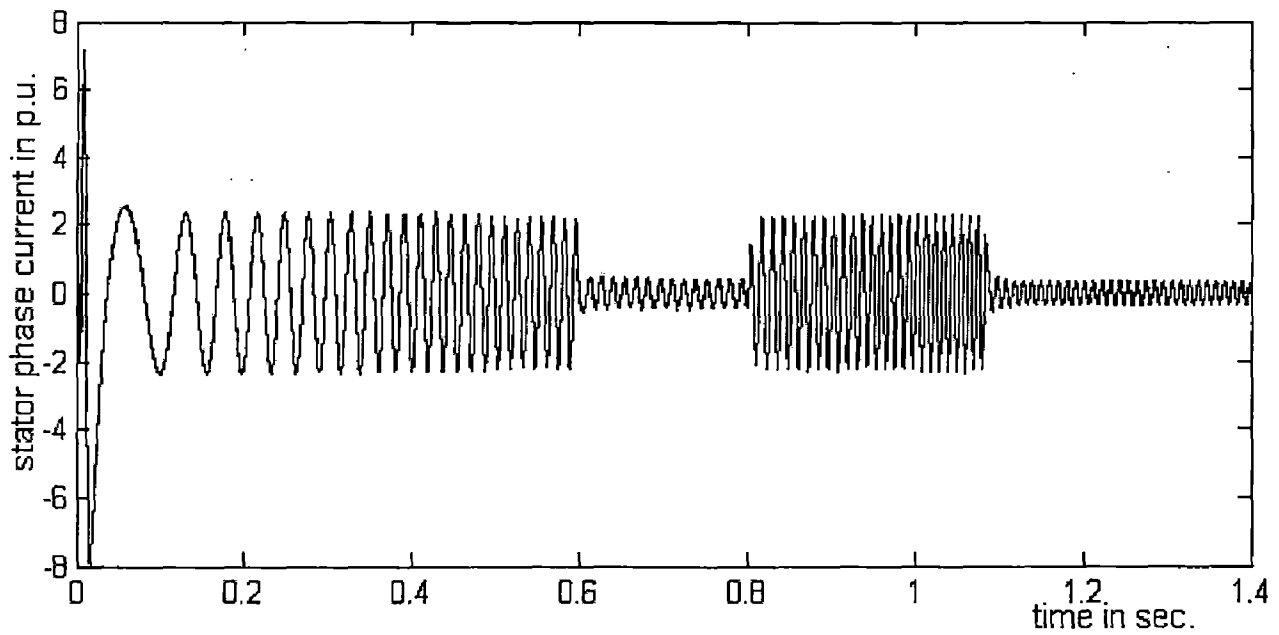


Fig. 5.24: Stator phase current (I_{as}) response when step change in speed above base speed.

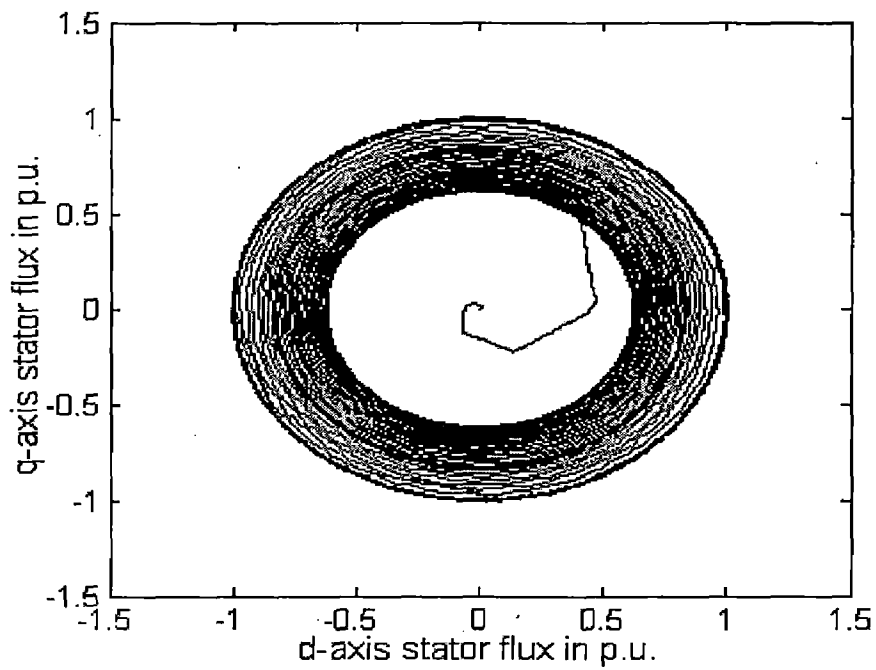


Fig. 5.25(a) : d-q Stator flux loci

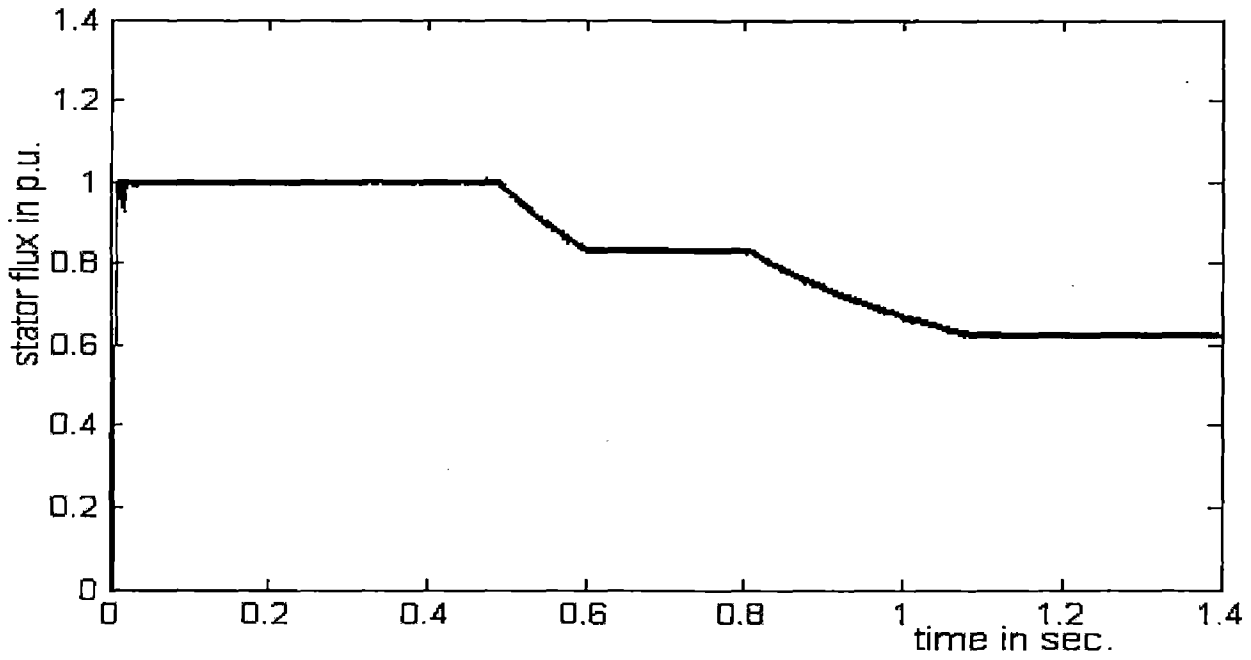


Fig. 5.25(b): Stator flux magnitude

Fig. 5.25: Stator flux response when step change in speed above base speed.

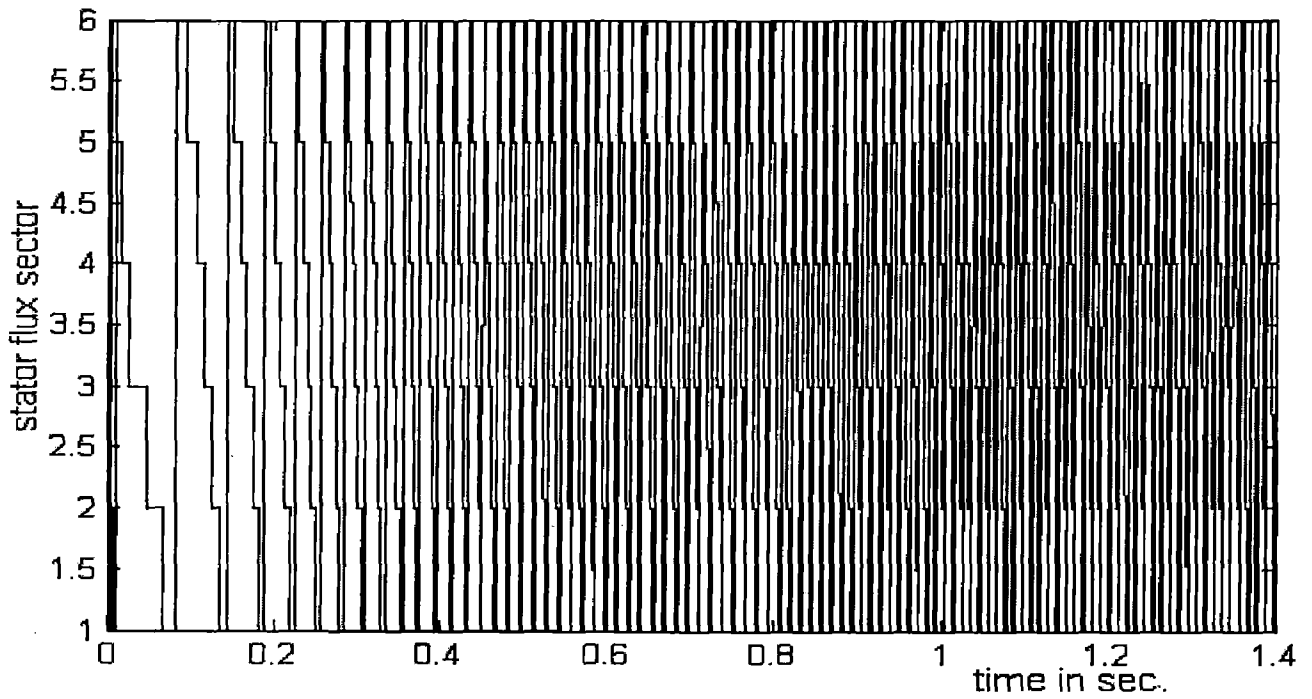


Fig. 5.26: Stator flux sector response when step change in speed above base speed.

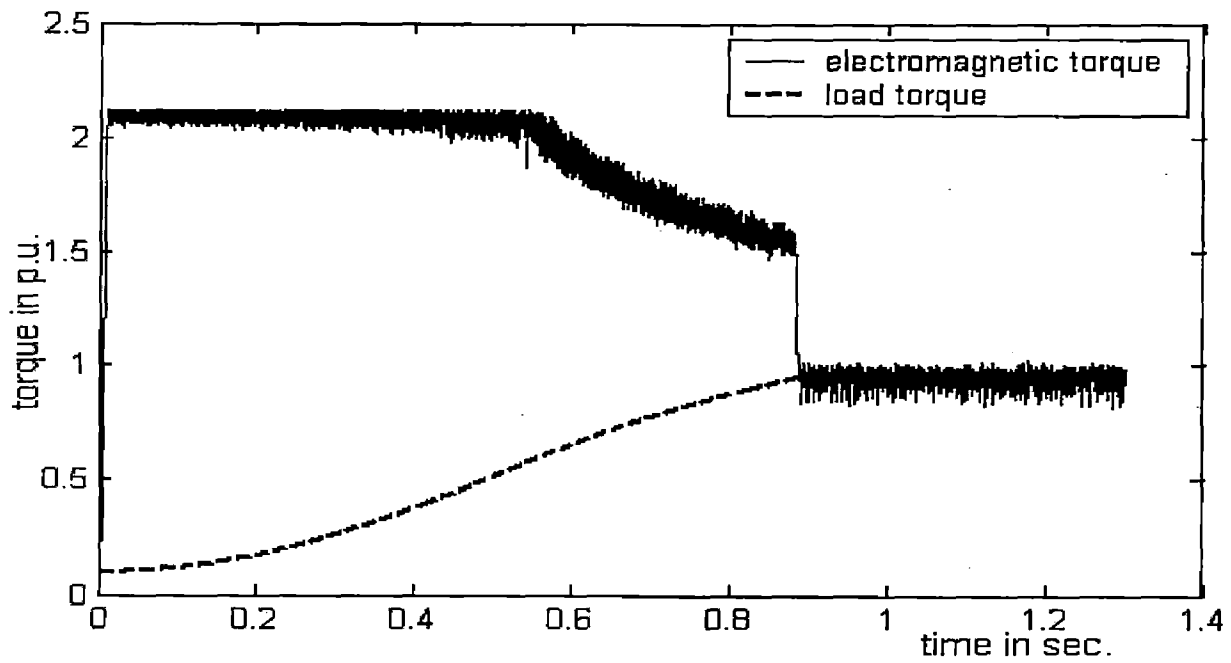


Fig. 5.27: Torque response under traction type load above base speed.

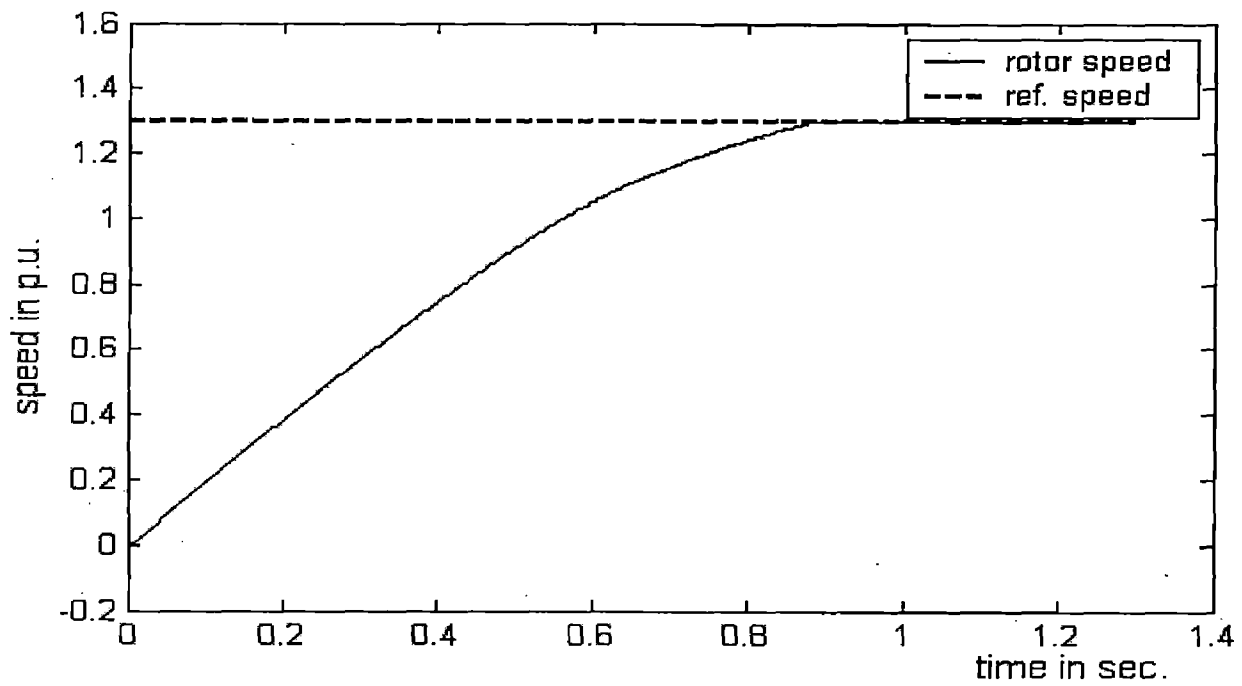


Fig. 5.28: Rotor speed response under traction type load above base speed.

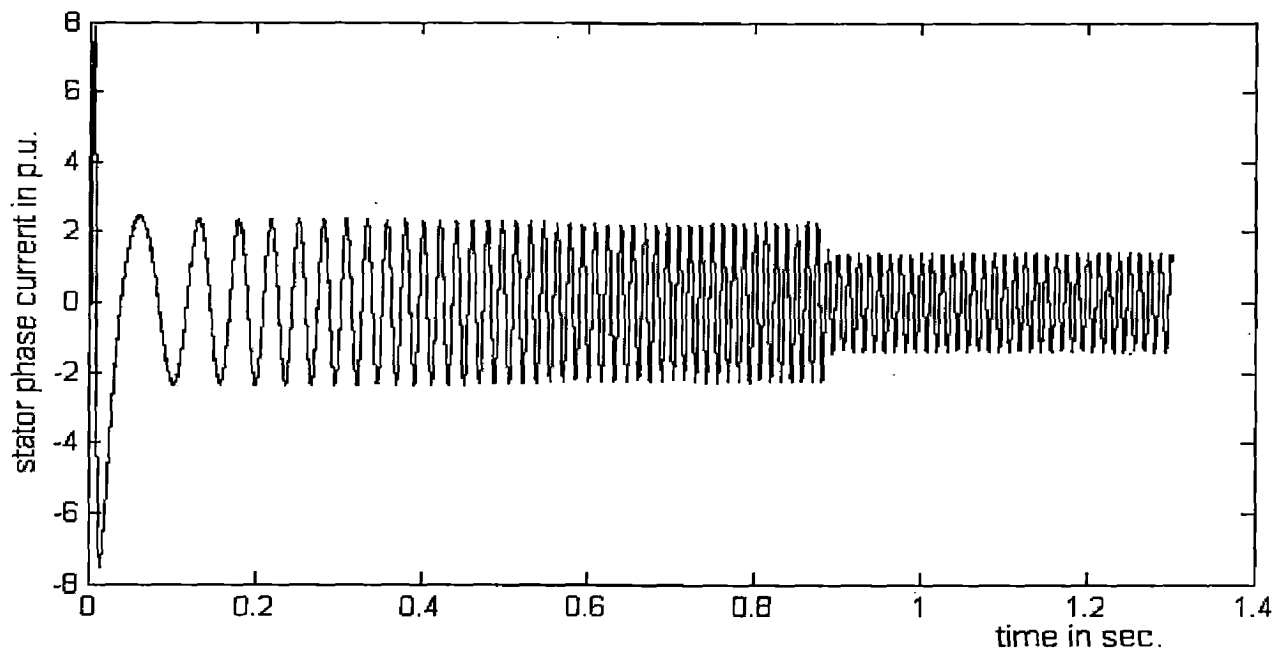


Fig. 5.29: Stator phase current (I_{as}) response under traction type load above base speed.

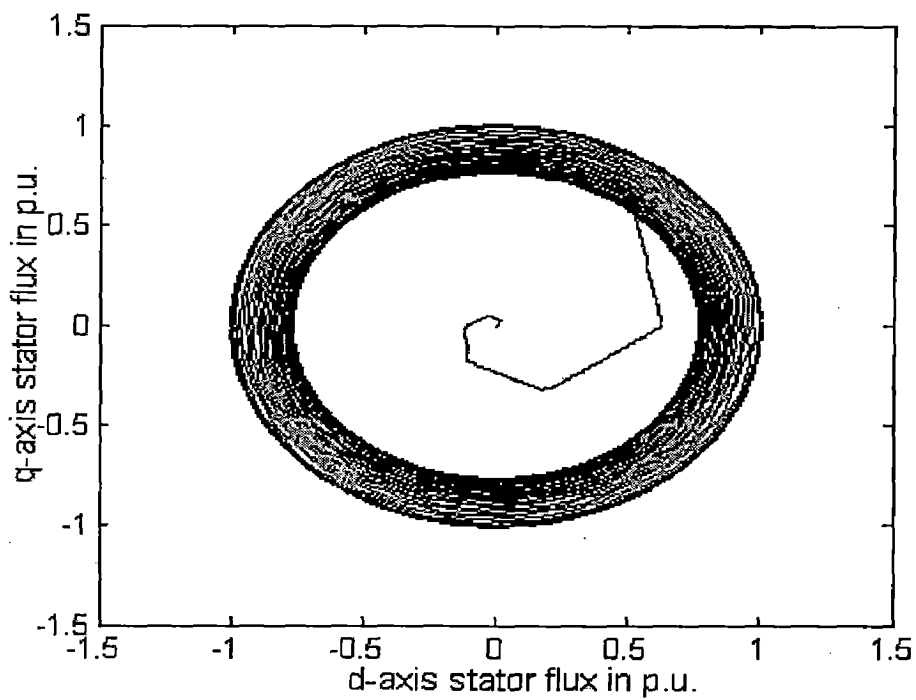


Fig. 5.30(a): d-q Stator flux loci

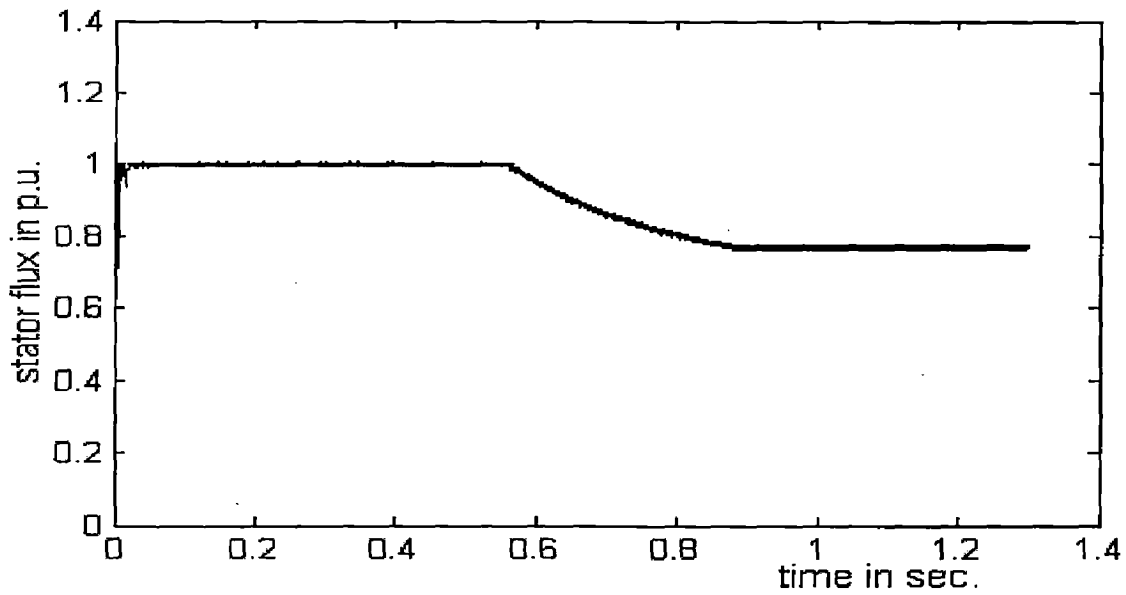


Fig. 5.30(b): Stator flux magnitude

Fig. 5.30 Stator flux response under traction type load above base speed.

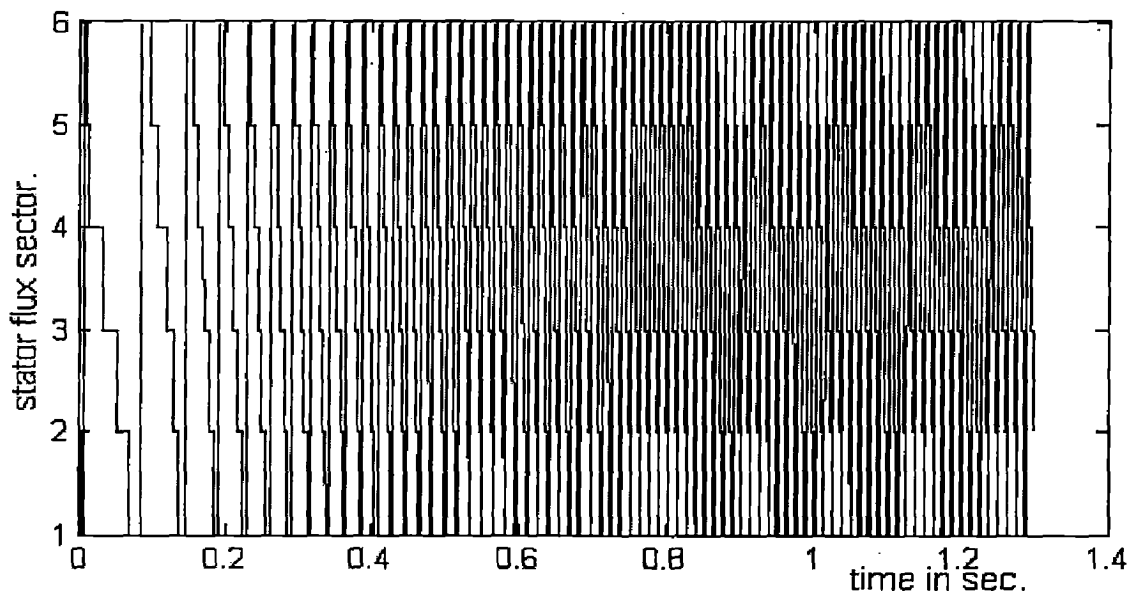


Fig. 5.31: Stator flux sector response under traction type load above base speed.

5.1.3 Traction type load

Fig 5.17 to Fig 5.31 show the simulation results when load is varied as

$$T_l = (0.6 * \omega_r * \omega_r + 0.1) \tag{5.2}$$

It show transient and steady state response of the induction motor characteristics like torque in Fig 5.22, speed in Fig 5.23, stator phase current Fig 5.24, stator flux in Fig 5.25 and stator flux sector in Fig 5.26. Here it is observed that stator phase current remain constant to its maximum value until motor speed become reference speed and then it obtain current corresponding to load torque. The electromagnetic torque and stator flux follow the constant torque characteristic up to base speed and after it constant power characteristic until steady state response is reached irrespective of load variation.

CHAPTER: 6

CONCLUSIONS AND SCOPE OF FURTHER WORK

6.1 CONCLUSIONS

In the present work, implementation of high performance direct torque control induction motor drive is presented that can be used in traction application.

The control of induction motor drive is discussed in both constant torque region and flux weakening region in different load condition and different speed reference. The proportional-integral controller is used as speed controller to provided fast response. In operation, the speed is sensed and error between reference speed and feedback speed is integrated in speed controller which sets the reference torque. Here we seen that flux and torque can be control separately only by selecting the inverter switching states according to the error of torque and flux.

It is well known that the principle of vector control of induction motor drive is to align the flux and torque current along the d-axis and q-axis of the reference frame, respectively. And therefore, the torque can be controlled by the associated current component, once the flux is kept constant. For this purpose a lot of precise calculation have to be done. In contrast, the fundamental ideal of direct torque control is to control both magnitude flux and torque with in associated error band. these control goals can be achieved by selecting the inverter switching states according to the error of torque and flux. Here it is also observed that stator current is indirectly control. Due to these feature direct torque control induction motor can be efficiently used in electric traction applications.

6.2 FURTHER WORK

In the present work, the performance of VSI fed induction motor is investigated for the traction applications by simulation in MATLAB. In future work the following work can be worked:

1. The hardware implementation of the given drive for three-phase induction motor.

2. Similar analysis can be performed with out using speed sensor.
3. Different type of switching control scheme with less torque ripple will be implemented[19][20].
4. The close loop of the drive can be controlled using microcontroller.

BIBLIOGRAPHY

- 1) T.G.Habetler, Deepakraj M. Divan, "Control Strategy for Direct Torque Control of Using Discrete pulse space Modulation", IEEE Trans. Ind. App. , vol. 27, no. 5, pp.893-901, Sept./Oct. 1991
- 2) T.G.Habetler, "Direct Torque Control of Using space Vector Modulation", IEEE Trans. Ind. App. , vol. 28, no. 5, pp.1045-1053, Sept./Oct. 1992.
- 3) R.J. Hill, "Electric railways traction part 1 Traction Drives with Three phase Induction motors", Power engineering journal, Vol.: 8, Issue:3, Feb. 1994 page47-56
- 4) R.J. Hill, "Electric railways traction part 2 Traction Drives with Three phase Induction motors", Power engineering journal, Vol.: 8, Issue:3, June 1994 page143-152
- 5) Y.A.Chapuis, C.Pelissou, D.Roya, "Direct Torque Control of an Induction Machine Under Square Wave Conditions", Industry Applications Conference, 1995. Thirtieth IAS Annual Meeting, IAS '95., Conference Record of the 1995 IEEE, Volume:1, 1995 Page: 343-349.
- 6) Y.A.Chapuis, D.Roya, J.Davoine, "Principles and implementation of Direct Torque Control by stator flux orientation of an Induction Motor", IEEE Applied Power Electronic conference and Exposition-Industry -Dallas, March 1995.
- 7) Domenico Casadei, Giovanni Serra and Angelo Tani, "Improvement of Direct Torque Control Performance by using a Discrete SVM technique", IEEE Trans. Ind. App., 1998

- 8) Jun-Koo Kang and Seung-Ki Sul, "New Direct Torque Control of Induction Motor for Minimum Torque Ripple and Constant Switching Frequency", IEEE Trans. Ind. App, Vol. 35, No. 5, Sept./Oct. 1999.
- 9) P.S.Bimbhra, "Power Electronics", third edition, Khanna Publishers, 1999 (Book)
- 10) G.K.Dubey, "Fundamental of Electric Drives", Second edition, Narosa Publisher House, 2001(Book)
- 11) P. C. Krause, "*Analysis of electric machinery*", McGraw-Hill, 2001.(Book)
- 12) Yen-Shin Lai and Jian-Ho Chen, " A New Approach to Direct torque control of induction motor for constant Inverter Switching Frequency and Torque Ripple Reduction", IEEE Transaction on energy conversion, vol. 16, NO. 3, Sept. 2001
- 13) Hu Hu, Yong Dong Li and Yi Zeng; "Direct torque control of induction motor for railway traction in whole speed range", IECON 02 [Industrial Electronics Society, IEEE 2002 28th Annual Conference of the]Volume 3, 5-8 Nov. 2002 Page(s):2161 - 2166 vol.3 .
- 14) Hu Hu Yongdong Li, "Application of induction motor Drive Based on DTC in railways Traction", IEEE Trans. Ind. App. 2002
- 15) Qu wenlong, Yang Yi, "Control strategies of direct torque control of induction motor applied to Traction", IEEE Trans. Ind. App., 2002
- 16) B.K. Bose, "Modern Power electronics and AC Drives", Published by Pearson Education (Singapore) pte, Ltd. Indian Branch, 2003 (Book)
- 17) R. Krishnan, "Electric motor drives, modeling, analysis and control", Prentice- Hall of India Private Limited, New Delhi-110001,2003 (Book)

- 18) Nik Rumzi Nik Idris, and Abdul Halim Mohamed Yatim, "Direct Torque Control of Induction Machines With Constant Switching Frequency and Reduced Torque Ripple", IEEE Trans. on industrial electronics, vol. 51, no 4, Aug. 2004
- 19) Idris, N.R.N.; Yatim, A.H.M.; Azli, N.A, "Direct Torque Control of Induction Machines With Constant Switching Frequency and improved stator flux estimation", Industrial Electronics Society, 2001. IECON '01. The 27th Annual Conference of the IEEE Volume 2, 29 Nov.-2 Dec. 2001 Page(s):1285 - 1291 vol.2
- 20) Petar R. Matic, Branko D. Blanusa and Slobodan N. Vukosavic, "A Novel Direct Torque and Flux Control Algorithm for the Induction Motor drive.", Electric Machines and Drives Conference, 2003. IEMDC'03. IEEE International Volume 2, 1-4 June 2003 Page(s):965 - 970 vol.2 .
- 21) <http://www.trainweb.org/railways/drives.html>
- 22) <http://www.drivetechinc.com/articles/IM98VC1.pdf>

APPENDIX-A

The Induction motor, selected for simulation, has specification as follow:

Induction motor Type	- Squirrel cage
Power	- 10 hp
Line-to-Line Voltage	- 220 V
Phase	- 3
Base frequency	- 60 Hz
Rotor resistance in p.u. (R_r)	- 0.0453
Stator resistance in p.u. (R_s)	- 0.0453
Rotor reactance at base frequency in p.u. (X_{lr})	- 0.0322
Stator reactance at base frequency in p.u. (X_{ls})	- 0.0775
Magnetizing reactance at base frequency in p.u. (X_m)	- 2.042
Inertia of rotor in p.u.(H)	- 0.5 sec.